Geomorphology 228 (2015) 382–397

Contents lists available at ScienceDirect

Geomorphology

journal homepage: www.elsevier.com/locate/geomorph

Geomorphology and weathering characteristics of erratic boulder trains on Tierra del Fuego, southernmost South America: Implications for dating of glacial deposits

Christopher M. Darvill *, Michael J. Bentley, Chris R. Stokes

Department of Geography, Durham University, South Road, Durham DH1 3LE, UK

ARTICLE INFO

Article history:
Received 5 May 2014
Received in revised form 3 September 2014
Accepted 6 September 2014
Available online 30 September 2014

Keywords:
Erratic boulder train
Supraglacial
Subglacial
Rock avalanche
Weathering
Cosmogenic nuclide exposure dating

ABSTRACT

Erratic boulder trains (EBTs) are a useful glacial geomorphological feature because they reveal former ice flow trajectories and can be targeted for cosmogenic nuclide exposure dating. However, understanding how they are transported and deposited is important because this has implications for palaeoglaciological reconstructions and the pre-exposure and/or erosion of the boulders. In this study, we review previous work on EBTs, which indicates that they may form subglacially or supraglacially but that large angular boulders transported long distances generally reflect supraglacial transport. We then report detailed observations of EBTs from Tierra del Fuego, southernmost South America, where their characteristics provide a useful framework for the interpretation of previously published cosmogenic nuclide exposure dates. We present the first comprehensive map of the EBTs and analyse their spatial distribution, size, and physical appearance. Results suggest that they were produced by one or more supraglacial rock avalanches in the Cordillera Darwin and were then transported supraglacially for 100 s of kilometres before being deposited. Rock surface weathering analysis shows no significant difference in the weathering characteristics of a sequence of EBTs, previously hypothesized to be of significantly different age (i.e., different glacial cycles). We interpret this to indicate that the EBTs are much closer in age than previous work has implied. This emphasises the importance of understanding EBT formation when using them for cosmogenic nuclide exposure dating.

1. Introduction

Erratic boulder trains (EBTs) are a poorly understood glacial geomorphological feature. These linear clusters of erratic boulders record the flow lines of former glaciers by pinpointing the parent rock from which they have originated (Kujansuu and Saarnisto, 1990; Evans, 2007) and have frequently been targeted for cosmogenic nuclide exposure dating (Jackson et al., 1997, 1999; McCulloch et al., 2005; Kaplan et al., 2007, 2008; Ward et al., 2007; Evenson et al., 2009; Vincent et al., 2010; Wilson et al., 2012). Consequently, they offer a valuable tool for reconstructing the nature and timing of former glacial advances.

Despite their importance to palaeoglaciology, these features are rarely reported in detail, and understanding their formation will help contextualise dating studies. This paper brings together previous literature on EBTs to assess how they form and presents detailed observations of examples from Tierra del Fuego, southernmost South America. The Tierra del Fuego EBTs make an excellent case study because they are well preserved and easily distinguishable. They have also been investigated using cosmogenic nuclide exposure dating, but the resultant ages can be interpreted in two quite different ways (McCulloch et al., 2005; Kaplan et al., 2007, 2008; Evenson et al., 2009). This study aims to test between these two opposing hypotheses by combining spatial and volumetric measurements with weathering proxies to gain a better understanding of EBT formation. In this way, we test the interpretation of cosmogenic nuclide exposure dates.

2. Definition and previous work on erratic boulder trains

The EBTs are a subset of dispersal trains, which includes any dispersal of a particular lithology by former ice flow (DiLabio, 1981, 1990; Dyke and Morris, 1988; Evans, 2007). However, whilst EBTs are linear clusters of boulders, other dispersal trains are not necessarily linear or clustered and can include a wide range of grain sizes, surficial and within glacial deposits. Given the lack of any previous compilation in the literature, we begin by providing a brief review of the limited number of detailed studies of EBTs, summarised in Fig. 1 and Table 1, focusing on their formation and dating. Likely other EBTs exist, but they are rarely reported in the literature and are often only given cursory mention in wider studies.

* Corresponding author. Tel.: +44 191 3341800.
E-mail address: christopher.darvill@durham.ac.uk (C.M. Darvill).

http://dx.doi.org/10.1016/j.geomorph.2014.09.017

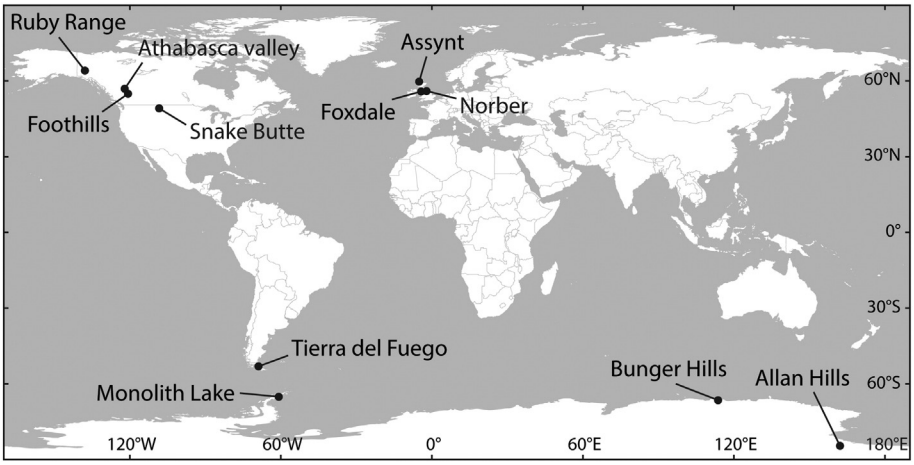

Fig. 1. Map showing the locations of erratic boulder trains reviewed in this paper (see Section 2).

2.1. Formation: subglacial versus supraglacial

No single model for the formation of EBTs exists, and it is possible that they can be formed in a variety of ways. This is not surprising given the reported variety in boulder size, train length, number of boulders, transport distance, and lithology (Table 1). Two hypotheses prevail: (i) subglacial entrainment and (ii) supraglacial debris.

The Norber EBT in England, Foxdale EBTs on the Isle of Man, Bunger Hills EBT and Allan Hills EBT in Antarctica, and Snake Butte EBT in the USA (see Fig. 1 and Table 1) are all interpreted to have formed subglacially. The Norber boulders have been transported laterally more than 1 km and 120 m vertically upward from their source lithology (Huddart, 2002; Wilson et al., 2012). Given that the ice flowed over the source outcrop (Vincent et al., 2010), we suggest that subglacial transport of the boulders is most probable (though the formation mechanism has not been investigated further). The two Foxdale boulder trains were interpreted to have been initially transported and deposited subglacially by ice flowing southeastward, but with subsequent ice flowing southwestward and dispersing the larger train subglacially across a broader area of the southern part of the island (Roberts et al., 2007). In the Bunger Hills, Augustinus et al. (1997) suggested that a lack of glacial polish or facetting on the boulders implied subglacial transport over only a very short distance, thereby explaining the limited extent of the EBT. Likewise, Atkins et al. (2002) considered the boulders of the Allan Hills EBT to have been eroded by plucking of the Beacon sandstone bedrock prior to subglacial dragging and deposition on the stoss side of a bedrock ridge. Knechtel (1942) suggested that striations and polished surfaces of boulders of the Snake Butte EBT resulted from transport at the base of ice flowing southeastward and that they were then deposited with ground moraine.

Table 1
Summary of the key characteristics of EBTs based on a review of the literature (NR = not reported).

EBT name	Location	Length of train(s)	Max. distance from source	Boulder diameter	Lithology	Suggested transport pathway	CNE dated?	Age	References
Foothills	Canada	>580 km	>580 km	1–41 m	Quartzite and pebbly quartzite	Supraglacial	^{36}Cl	18–12ka	Stalker (1956); Mountjoy (1958); Stalker (1976); Jackson et al. (1997); Jackson et al. (1999); Jackson and Little (2004)
Athabasca valley	Canada	ca. 70 km	ca. 120 km	Up to 1 m	Metamorphic schist	Supraglacial	–	–	Roed et al. (1967)
Ruby Range	Canada	ca. 5 km	ca. 5 km	Some >1.5 m	NR	NR	^{10}Be	54–51 ka	Ward et al. (2007)
Snake Butte	USA	ca. 79 km	ca. 80 km	Up to 23 m	Shonkinite	Subglacial?	–	–	Knechtel (1942)
Assynt	Scotland	9–14 km (4 trains)	>9 km	NR	Sandstone	NR	–	–	Lawson (1990); Lawson (1995)
Norber	England	>1 km	>1 km	Up to 4 m	Greywacke	Likely subglacial over a short distance	^{36}Cl	22–17 ka	Davis (1880); Goldie (2005); Huddart (2002); Vincent et al. (2010); Wilson et al. (2012)
Foxdale	Isle of Man	Up to 1 km	≤2 km	Up to 1 m	Granite	Subglacial	–	–	Roberts et al. (2007); Roberts (*pers. comm.*)
Bunger Hills	Antarctica	Up to 4 km?	≤4 km	NR	Dolerite	Subglacial but only a short distance	–	–	Adamson and Colhoun (1992); Augustinus et al. (1997)
Allan Hills	Antarctica	Up to 3 km?	≤3 km	Up to 3 m	Sandstone	Subglacial	–	–	Atkins et al. (2002)
Monolith Lake	Antarctica	ca. 9 km	ca. 12 km	Up to 5 m	Hyaloclastite	Likely supraglacial	–	–	Davies et al. (2013)
Tierra del Fuego	Chile/Argentina	4–15 km (4 trains) 95 km total	ca. 250 km	Up to 21 m	Granodiorite	Supraglacial	^{10}Be ^{26}Al ^{36}Cl	222–15 ka	Darwin (1841); Meglioli (1992); Coronato et al. (1999); Bentley et al. (2005); McCulloch et al. (2005); Kaplan et al. (2007); Kaplan et al. (2008); Evenson et al. (2009); This study

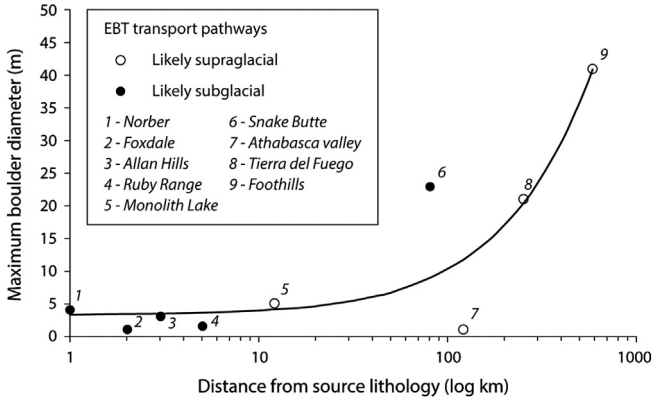

Fig. 2. Maximum boulder diameter plotted against the maximum distance of boulders from their source lithology (note the log scale), as reported in studies of EBTs (labelled as per Table 1). Our review of the literature suggests that EBTs consisting of larger boulders (>5 m) transported greater distances (>10 km) are more likely to have been transported supraglacially. The Snake Butte EBT is an exception to this pattern; Knechtel (1942) inferred subglacial transport of these boulders. Of the reported studies, lithology does not appear to play a key role in determining the preservation of boulder trains through supraglacial or subglacial transport.

In contrast, the Foothills EBT and Athabasca Valley EBT in Canada, Monolith Lake EBT in Antarctica, and Tierra del Fuego EBTs in Chile/Argentina are all suggested to have formed from material being deposited onto ice and then transported supraglacially. The Foothills boulder train formed in a medial ice position as two lobes converged around a nunatak and show no signs of subglacial transport (Jackson and Little, 2004). Similarly, the friable nature of the Monolith Lake boulders means that they are only likely to have survived if transported supraglacially (Davies et al., 2013). Meglioli (1992), Bentley et al. (2005), McCulloch et al. (2005), and Evenson et al. (2009) all noted the tight distribution, large size, angularity, and monolithology of the boulders on Tierra del Fuego, which are unlikely to have survived subglacial erosion and are instead indicative of supraglacial transport (Evenson et al., 2009).

The transport pathway has important implications for the likely exposure and depositional history of a boulder train. Too few detailed studies of EBTs exist to be able to clearly define their formation based on physical characteristics. However, our synthesis of previously published data suggests an apparent trend between transport distance, boulder size, and the proposed transport pathway (Fig. 2), with those moved greater distances (e.g. >~10 km) more likely to have been transported supraglacially. The relationship with boulder size is

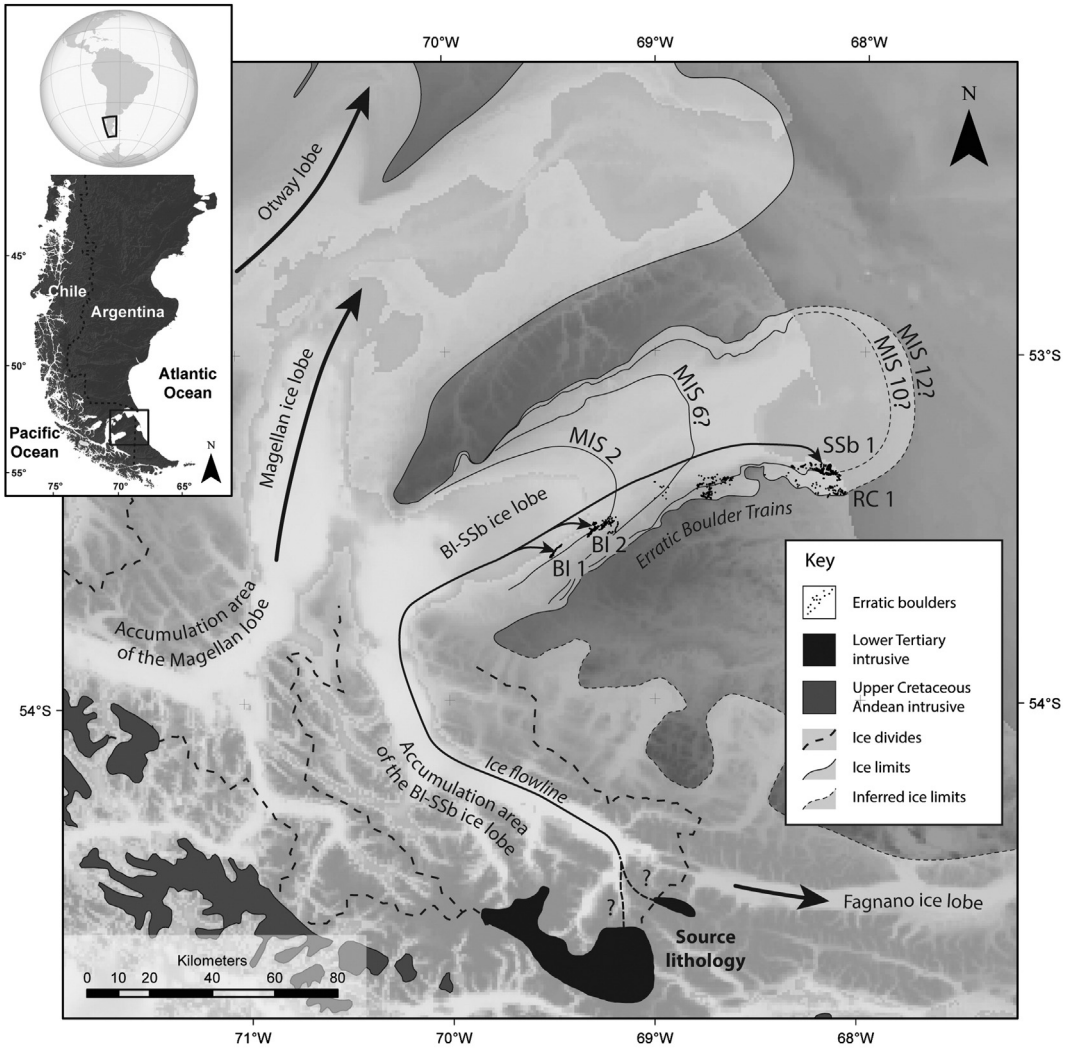

Fig. 3. The location of the study area, showing the extent of former ice lobes in southernmost South America. Thick dashed lines indicate inferred ice divides, and thin lines show the outermost limit of ice lobes based on geomorphology mapped by Darvill et al. (2014) or inferred (dashed) from the literature. For the Bahía Inútil–San Sebastián (BI–SSb) ice lobe, the hypothesised limits and their ages are shown to illustrate how the EBTs relate to them. All other ice lobes are shown at maximum extent, though this does not imply that they advanced or retreated to these limits at the same time. A former flow line from the source lithology in the Darwin Cordillera to the EBTs on Tierra del Fuego is illustrated. The two possible origins of the granodiorite lithology are shown (from Natland et al., 1974), but only the lower Tertiary intrusive unit outcrops in the former accumulation area of the BI–SSb ice lobe.

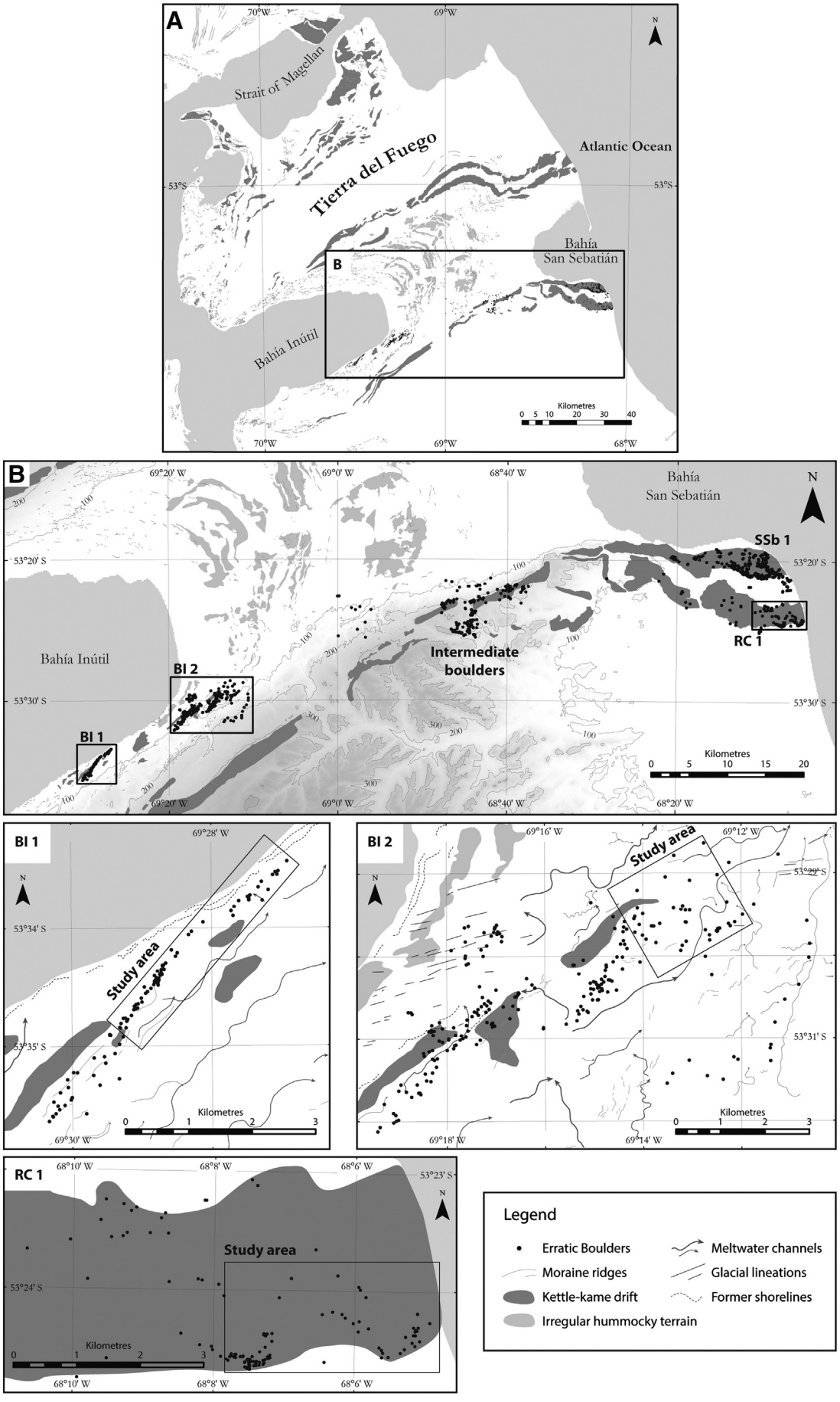
A
70°W
69°W
68°W
53°S
N
Strait of Magellan
Tierra del Fuego
Atlantic Ocean
Bahía
San Sebatián
Bahía Inútil
B
Kilometres
0 5 10 20 30 40
B
69°20' W
69°0' W
68°40' W
68°20' W
53°20' S
53°30' S
Bahía
San Sebatián
N
SSb 1
RC 1
Bahía Inútil
BI 2
BI 1
Intermediate
boulders
100
200
300
Kilometres
0 5 10 15 20
BI 1
69°28' W
69°30' W
53°34' S
53°35' S
Study area
Kilometres
0 1 2 3
BI 2
69°16' W
69°12' W
69°18' W
69°14' W
53°29' S
53°31' S
Study area
Kilometres
0 1 2 3
RC 1
68°10' W
68°8' W
68°6' W
53°23' S
53°24' S
Study area
Kilometres
0 1 2 3
Legend
Erratic Boulders
Moraine ridges
Kettle-kame drift
Irregular hummocky terrain
Meltwater channels
Glacial lineations
Former shorelines

unsurprising given the association between transport pathway and boulder erosion (Boulton, 1978), but is important in the context of erratic dispersal more generally. For example, the principles of 'half-distance' transport (Salonen, 1986) and concentration peaks (DiLabio, 1981, 1990; Boulton, 1996) may better relate to subglacial EBTs, whereas supraglacial EBTs are also controlled by the maximum transport distance and the preservation potential of the boulders.

2.2. Cosmogenic nuclide exposure dating

The EBTs are useful targets for cosmogenic nuclide exposure dating, with the added benefit of being able to trace the source and transport pathway of the samples. The Foothills boulder train in Canada was dated using ^{36}Cl by Jackson et al. (1997, 1999), yielding dates of 18–12 ka and demonstrating the limits of the Laurentide Ice Sheet during its Last Glacial Maximum (LGM). The dates implied a maximum transport time of ca. 3 ka (<17% of the total exposure time; Jackson and Duk-Rodkin, 1996; Jackson et al., 1997) and yielded one anomalously old age of ca. 53.3 ka, which Jackson et al. (1997) ascribed to pre-exposure.

The Norber boulder train in England was also dated to around 22–17 ka using ^{36}Cl, which helped establish the timing of deglaciation in the region (Vincent et al., 2010; Wilson et al., 2012). The ^{10}Be dates from the Ruby Range boulder train in Canada were clustered and suggested that the train was deposited during the penultimate glacial episode, with dates of 54–51 ka (Ward et al., 2007). The authors suggested no significant influence of inheritance given that the same pre-exposure prior to deposition of all four samples is unlikely (Ward et al., 2007), and subglacial transport of the Norber and Ruby Range boulders may have removed any inheritance signal. Statistical modelling of supraglacial erosion and transport of boulders has also suggested that these processes can yield dateable inheritance signatures in erratic boulders (Applegate et al., 2010, 2012; Heyman et al., 2011).

As noted above, the Tierra del Fuego EBTs have been targeted for cosmogenic nuclide exposure dating (McCulloch et al., 2005; Kaplan et al., 2007, 2008; Evenson et al., 2009). The established regional age model for the timing of glaciations implies that a series of four glacial limits are successively less extensive (i.e., 'nested') and correspond to different glacial cycles: MIS 12, 10, 6, and 2 (Fig. 3). This is based on palaeomagnetism, uranium-series dating, correlation between marine terraces, and relative weathering indices and augmented by radiocarbon, amino acid racemization, and tephra dating of the younger limits (Meglioli, 1992; Coronato et al., 2004; Rabassa, 2008; Rabassa et al., 2011; and references therein). Published cosmogenic nuclide exposure dates from two EBTs on the MIS 2 (LGM) limit close to Bahía Inútil cluster around 20 ka (Figs. 4 and 5) and agree well with radiocarbon dates of deglaciation in the region (Heusser, 2003; McCulloch et al., 2005; Kaplan et al., 2008; Hall et al., 2013). However, two EBTs on the outer two limits yielded dates significantly younger than expected, dominantly between 30 and 15 ka for the putative MIS 12 limit ($n = 7$) and two dates of 24 and 222 ka for the putative MIS 10 limit (Kaplan et al., 2007; Evenson et al., 2009).

Our review of the literature highlights that EBTs can form in different ways, with different erosion, transport, and depositional histories. For supraglacial EBTs, this can result in incomplete erosion of inherited nuclide concentrations, which is important to understand if using the features for cosmogenic nuclide exposure dating.

2.3. This study

Kaplan et al. (2007) suggested that the occasional older dates for the EBTs on Tierra del Fuego were closer to the true age of the glacial limits and proposed that intense, episodic exhumation and/or erosion of the EBTs resulted in the samples yielding anomalously young ages (i.e., they are 'old' boulders that were exhumed; Fig. 6). However, an alternative hypothesis, not previously considered, is that all of the EBTs in Tierra del Fuego were deposited during the last glacial cycle (i.e., they are 'young' boulders; Fig. 6), and occasional samples are anomalously old owing to inheritance. The 'old' hypothesis fits with the established age model but requires intense physical exhumation and erosion to explain the dates (Kaplan et al., 2007). The 'young' hypothesis does not require such extreme processes but questions the established age model and implies that ice was much more extensive during the last glacial cycle. This study tests between these two opposing hypotheses, and a summary of the expected weathering characteristics that might be found under these two different scenarios is given in Table 2.

3. Methods

3.1. Mapping and sampling

We began by mapping all erratic boulders in the study area and then selected a sample of 150 boulders from three of the EBTs to compare trains hypothesised to be of similar and differing ages (Fig. 3). Many of the boulders are sufficiently large and clear against the surrounding landscape for them to be mapped from remote imagery, so a map was produced to show their distribution using a combination of remote sensing analysis and field-checking. Aerial photographs from the Servicio Aerofotométrico de la Fuerza Aérea de Chile were used where possible as well as Google Earth™ imagery (version 7). Field-checking verified the broad spread of mapped boulders, and the locations of the 150 sampled boulders were recorded using a handheld Magellan eXplorist 610 GPS device. All boulders within a given area were sampled provided they were >2 m in height. This was to avoid the effects of snow/vegetation cover and variable erosion on smaller boulders and to avoid the chances of sampling fragments that may have broken off subsequent to deposition. Boulders were described in terms of basic lithology, surface appearance, and setting.

3.2. Size approximation, angularity, and appearance

Boulders varied in size and accessibility, so boulder dimensions and volume were estimated using eight photographs taken around each boulder at roughly equal bearings. All photographs included a 1-m measuring-staff that was later used to gauge boulder height, width, and depth. Volume was then calculated in three ways to give approximate upper, middle, and lower values (supplementary material: SM1.2). Boulder angularity was recorded using a visual scale (Benn, 2004) and a relative measurement technique (Kirkbride, 2005; SM1.1). The surficial characteristics and lithology of the boulders were also noted.

3.3. Schmidt hammer

The Schmidt hammer has been used to measure rock-surface hardness as an indicator of the amount of time that rock has been exposed to subaerial processes (Matthews and Owen, 2010; see SM1.4). Rebound values (*R*-values) produced by the impact of the hammer decline with increased rock-surface weathering, and so can be used as a relative measure of exposure history (McCarroll, 1991; McCarroll and Nesje, 1993; Nesje et al., 1994; Goudie, 2006; Shakesby et al., 2011). We used an N-type Schmidt hammer to analyse 50 boulders from two of the boulder trains thought to be from different glacial cycles (BI 1 and RC 1). Fifty Schmidt hammer blows were recorded per boulder, with a total of 2500 blows

Fig. 4. (A) Simplified overview of the glacial geomorphology from Darvill et al. (2014) for Tierra del Fuego. (B) Detailed glacial geomorphological maps showing the boulders mapped in this study on Tierra del Fuego. From our mapping, the boulders clearly form EBTs (rather than simply being boulders on moraines): the trains cut across the moraine morphology, form isolated discrete clusters, and are not found on equivalent moraines to the north. Boxes in the overview map are shown enlarged below — these three boulder trains are examined in this study. The sampled boulders are highlighted within each respective EBT.

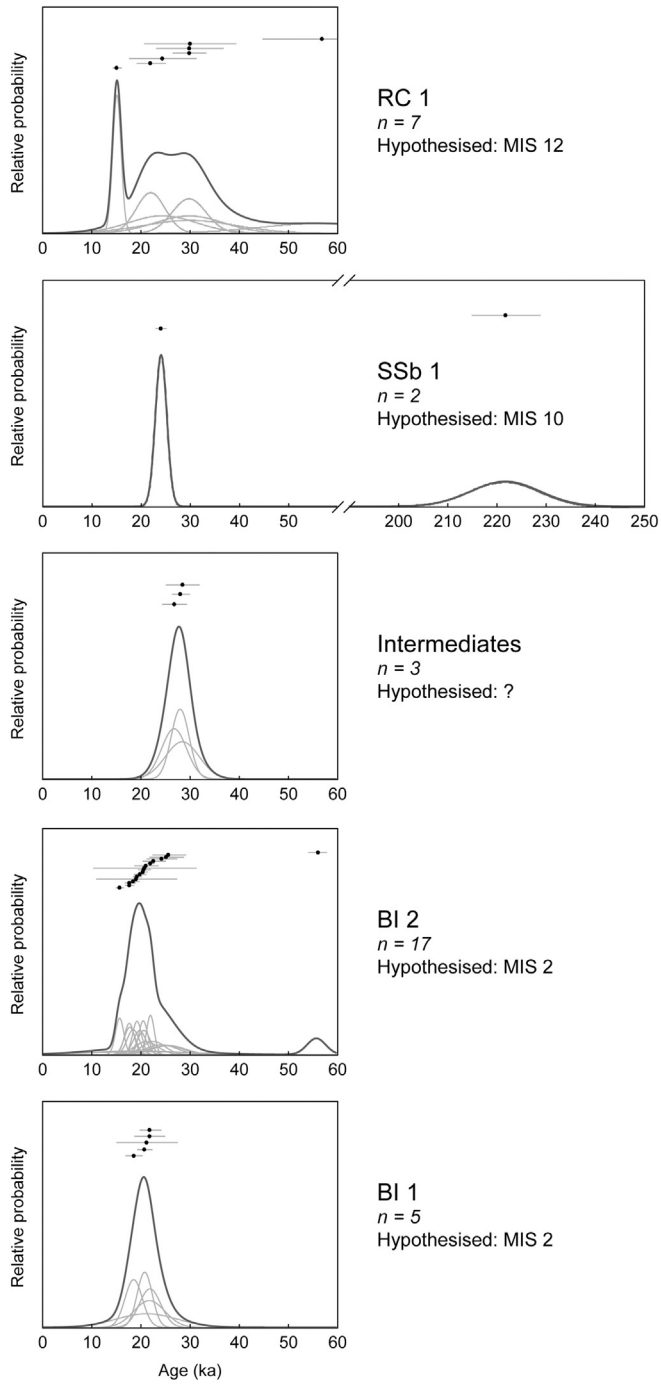

Fig. 5. Previous ^{10}Be cosmogenic nuclide exposure dates from the boulder trains, as mean ages with standard errors (plotted in age order) and as probability plots; recalculated from the original data of McCulloch et al. (2005), Kaplan et al. (2007, 2008), and Evenson et al. (2009); and using the production rate of Putnam et al. (2010) and the scaling model of Lal (1991) and Stone (2000). Note the substantial difference between the cosmogenic nuclide exposure dates and the hypothesised ages for RC 1 and SSb 1.

per boulder train (5000 blows in total). On each boulder, 10 blows were recorded per face (approximately: north, east, south, west, and top) to explore whether aspect is a control on rock-surface weathering.

3.4. Profile gauge

Rock surface roughness can be used to compare the effects of weathering where it is assumed that initial surface texture was roughly the same (McCarroll and Nesje, 1993, 1996). This can then be used as an indicator of the relative time that a rock surface has been exposed to weathering processes. A profile gauge is a quick and easy tool for measuring rock surface roughness (McCarroll and Nesje, 1996), and we used a 25-cm gauge consisting of 250 × 1 mm independent pins to sample planar rock surfaces (SM1.3). The gauge was pressed firmly against the surface and then traced onto graph paper in the field and later digitised. Pin positions were recorded every 8, 16, 24 and 32 mm to evaluate different roughness wavelengths. We measured roughness profiles for 50 boulders in three boulder trains (BI 1, BI 2, and RC 2). Five profiles were recorded per boulder, making a total of 250 profiles per boulder train (750 profiles in total). On each boulder, one profile was recorded per face (approximately: north, east, south, west, and top) to show whether roughness varied with aspect.

4. Results

4.1. Distribution

We mapped a total of 1248 boulders and distinguished four EBTs. From innermost (ice-proximal) to outermost (ice-distal), these are: BI 1, BI 2, SSb 1, and RC 1 (Fig. 4). In addition, a large spread of boulders lies between Bahía Inútil and Bahía San Sebastián (intermediates in Fig. 4B). These are dispersed rather than tightly clustered and so are not classed as an EBT for the purposes of our study. However, we highlight that these intermediate boulders bridge the gap between BI 1/BI 2 and SSb 1/RC 1. It was not possible to access the SSb 1 EBT or some of the intermediate boulders for field-checking or analysis, but both were sampled for cosmogenic nuclide exposure dating by Kaplan et al. (2007). A summary of the characteristics of the boulder trains is given in Table 3 and example photos are given in Fig. 7.

4.2. Volume characteristics

The total volume of rock within the measured boulders in BI 1, BI 2, and RC 1 combined is >22,000 m^3, within which the total volume of BI 1 is >5000 m^3, BI 2 is >14,000 m^3, and RC 1 is >2000 m^3 (Fig. 8). The largest boulders were in BI 2, with three boulders exceeding 1000 m^3. Of all boulders sampled, only one was found to be taller than it was wide, and we interpret this to indicate that almost all boulders are stable and 'at rest'. Several examples of 4–6 near-consecutive boulders were found to increase in volume down-ice (Fig. 8). This is masked in the field by scattered smaller boulders, and the pattern is least distinct in BI 2 where boulders are more dispersed. However, we suggest that these trends are real because they cannot be explained by measurement uncertainty or by changing the point from which EBT distance is measured.

4.3. Angularity

Little difference in angularity was recorded between boulder trains, and all showed a dominance of angular or subangular boulders, supported by RA values of 64% for BI 1/BI 2 and 54% for RC 1 (see Fig. 9).

4.4. Rock surface hardness

The Schmidt hammer *R*-values were corrected for the angle at which the Schmidt hammer was held and for instrumental drift (SM1.4). The total mean *R*-values for the two boulder trains are 43.6 ± 19.9 for BI 1 and 37.7 ± 19.7 for RC 1 (Fig. 10), and the means of different aspect faces also show consistently lower *R*-values for RC 1 than BI 1, in the range of 2.8–8.4. A Mann–Whitney U test reveals a statistical difference between the median values of the two EBTs at the 0.95 significance level ($p = <0.05$), when comparing total values and for each of the aspect faces.

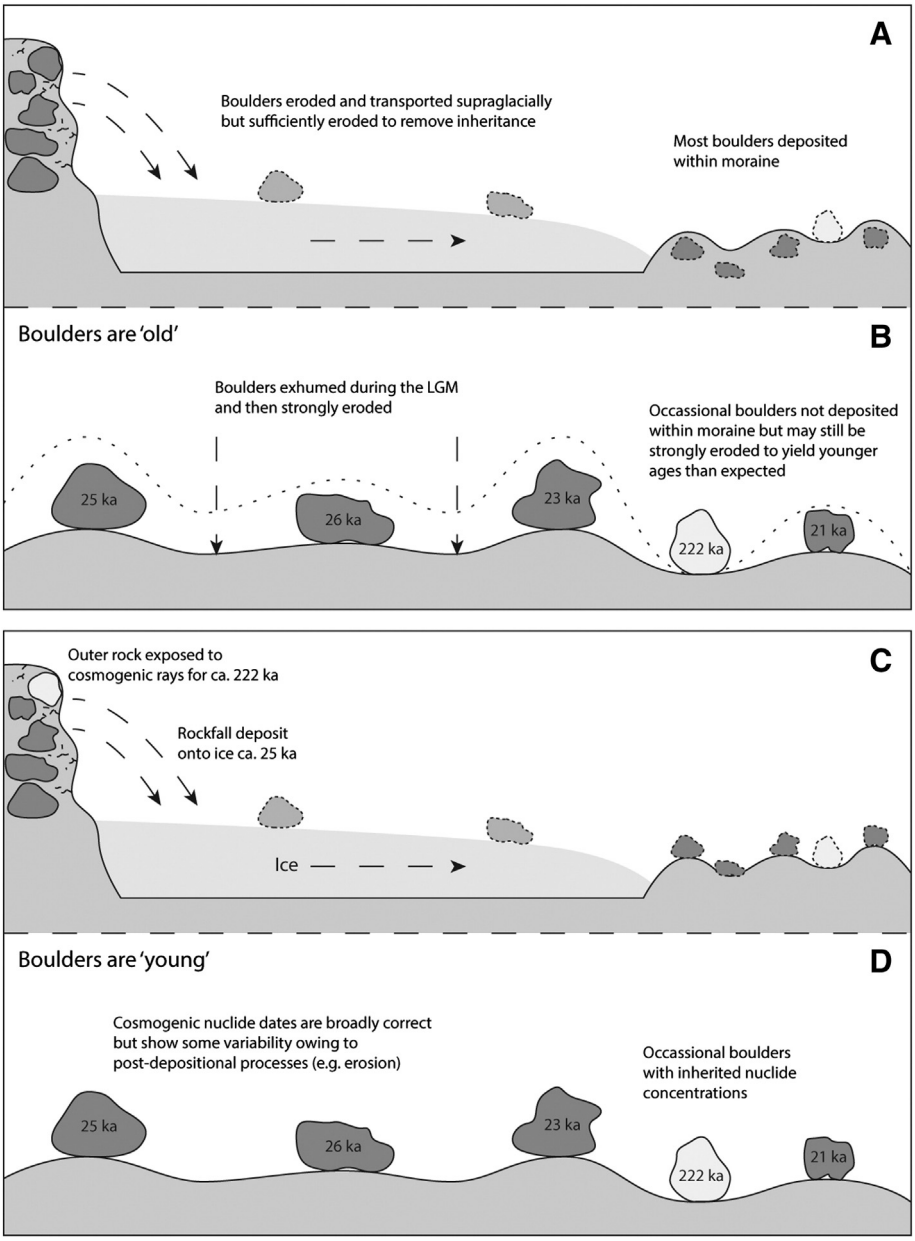

Fig. 6. The different cosmogenic nuclide exposure dates from the RC 1 and SSb 1 boulders on Tierra del Fuego can be explained by two different hypotheses. (A) and (B) Illustrate the first hypothesis, proposed by Kaplan et al. (2007), which suggests that the majority of the boulders were exhumed and eroded subsequent to deposition, yielding anomalously young ages. (C) and (D) Illustrate the second hypothesis, proposed in this study, which suggests that occasional boulders may be anomalously old owing to inheritance because they were not sufficiently eroded by supraglacial transport. In this case, the majority of the cosmogenic nuclide exposure dates are a better representative of the age of the EBTs.

4.5. Rock surface roughness

Following McCarroll and Nesje (1996), we present our roughness data in two ways. Index A uses the standard deviation of measurements and removes the influence of rock surface slope, whereas root mean square (RMS) represents roughness more accurately as deviation from the mean but will be affected by surface curvature (SM1.3). The profile gauge was used on all three boulder trains, and a strong correlation was found between Index A and RMS values (Fig. 11), indicating that surface curvature did not affect the roughness results. Consequently, RMS values are used to assess differences in surface roughness (Fig. 11). Reducing the wavelength reduces the mean roughness and spread of values, but McCarroll and Nesje (1996) suggested that lower wavelengths were unlikely to capture true surface roughness. We found that the greatest rock crystal size was generally >20 mm; hence we focus on the 32-mm wavelength data. The different number and spacing of data points along the profiles when the wavelength was varied did not affect the mean results, suggesting that the results indicate actual changes in roughness and are not caused by sampling strategy.

The total mean values for the three boulder trains are 2.4 ± 1.8 mm for BI 1, 2.3 ± 1.6 mm for BI 2, and 2.8 ± 2.3 mm for RC 1 at the 32-mm wavelength (Fig. 11). Like the Schmidt hammer data, patterns exists within the roughness results, with RC 1 consistently showing greater roughness – mean values 0.19–0.64 mm greater than the lowest mean value from BI 1 or BI 2 – for the total and different aspect faces. A Mann–Whitney U test shows a statistical difference between the total median values of all three EBTs at the 0.95 significance level ($p = <0.05$). Likewise, some, but not all, of the aspect faces also show a statistical difference when comparing all three of the EBTs, and this applies when comparing BI 1 and BI 2 as well as BI 1/BI 2 and RC 1.

Table 2
Age and likely weathering characteristics for the Tierra del Fuego EBTs.

	Boulder train		
Properties	BI 1/BI 2	RC 1 if 'old'[a]	RC 1 if 'young'[b]
Hypothesised age	20 ka[c]	ca. 450 ka[c]	30–20 ka[c]
Cosmogenic ages	ca. 20 ka[d]	ca. 30–15 ka[e]	ca. 30–15 ka[e]
Nature of erosion	Possibly some erosion	Intense exhumation and erosion[f]	Possibly some erosion
Likely agents of erosion	Wind erosion, frost action, dissolution, mild salt-spray weathering	Wind erosion, frost action, dissolution, salt-spray weathering	Wind erosion, frost action, dissolution, salt-spray weathering
Possible weathering rates	0.5–12 mm ka^{-1}[g]	>25 mm ka^{-1}[h]	0.5–12 mm ka^{-1}[g]
Likely surface erosion	≤240 mm[i]	500–>11,250 mm[j]	≤360 mm[k]
Likely erosional difference compared to BI 1/BI 2	0 mm	260–>11,010 mm	≤120 mm
Roughness compared to BI 1/BI 2	N/A	Significantly rougher	Possibly slightly rougher or the same
Hardness compared to BI 1/BI 2	N/A	Significantly weaker	Possibly slightly weaker or the same

[a] As hypothesised by Kaplan et al. (2007).
[b] As hypothesised in this study.
[c] Approximate ages, based on Meglioli (1992); Kaplan et al. (2007, 2008).
[d] McCulloch et al. (2005); Kaplan et al. (2008); Evenson et al. (2009).
[e] Kaplan et al. (2007); Evenson et al. (2009).
[f] Kaplan et al (2007).
[g] Kaplan et al. (2005) calculated apparent erosion rates of roughly 0.5 to 2.5 mm ka^{-1} over >760 ka for boulders deposited by the Lago Buenos Aires lobe in northern Patagonia. Kaplan et al. (2007) calculated apparent erosion rates of roughly 5 to 12 mm ka^{-1} over ca. 50–120 ka for boulders deposited by the Río Gallegos lobe in southern Patagonia.
[h] Apparent erosion rate estimated by Kaplan et al. (2007).
[i] Assuming up to 12 mm ka^{-1} erosion over 20 ka.
[j] Assuming >25 mm ka^{-1} erosion following rapid exhumation at 20 ka or continuous erosion at >25 mm ka^{-1} over 450 ka. Kaplan et al. (2007) suggested that continuous erosion is unlikely given preservation of original surface geomorphology, so the amount of erosion is probably between these two end members.
[k] Assuming up to 12 mm ka^{-1} erosion over up to 30 ka.

5. Discussion

5.1. Source

Kaplan et al. (2007) and Evenson et al. (2009) described the boulders from BI 1, BI 2, and RC 1 as hornblende granodiorites. The only source for this lithology is a small area of the Cordillera Darwin mountain range (Fig. 3), where lower Tertiary intrusive units outcrop within the former glacial accumulation area (Natland et al., 1974; Nelson et al., 1980; Evenson et al., 2009). This source suggests that the Bahía Inútil–San Sebastián (BI–SSb) ice lobe originated from the central Cordillera Darwin to the south. It also helps to position the ice divide between the BI–SSb and Fagnano ice lobes at peak glaciation; and the presence of supraglacial rock debris on Tierra del Fuego implies that granodiorite nunataks existed within the central Cordillera Darwin during peak glaciation. Thus, peak ice thickness could not have exceeded around 2500 m, which acts as a constraint on ice cap reconstructions.

The large boulders in Tierra del Fuego (up to 1000 m^3) are unlikely to have been transported subglacially given that erosion during the distance from their source (ca. 250 km) should have considerably reduced their size (Fig. 2). Furthermore, our data show that the boulders are dominantly angular or subangular. So many angular boulders up to 21 m in diameter are unlikely to have been transported beneath the ice over such a long distance. We found no evidence of subglacial abrasion (e.g. polishing or striae), and the angularity of the boulders suggests that such signs have not been removed by weathering. A similar conclusion was reached by Evenson et al. (2009). As such, the most likely formation mechanism is supraglacial debris at the source location in the Cordillera Darwin.

Meglioli (1992), Bentley et al. (2005), McCulloch et al. (2005), and Evenson et al. (2009) all noted the tight distribution, large size,

Table 3
The spatial characteristics and geomorphological context of the EBTs on Tierra del Fuego.

EBT	No. boulders mapped	Approx. train length (km)	Approx. train width (km)	Approx. train height (m asl)	Spatial distribution	Geomorphological context	Hypothesised ages
BI 1	98	5.5	0.5	50–70	A highly linear train extending to the coast of Bahía Inútil.	On a moraine belt, parallel to meltwater channels and with one meltwater channel dissecting it.	MIS 2
BI 2	238	11.0	7.5	60–220	Elements of linearity, but spread over a wider area than BI 1. May consist of more than one EBT, but not possible to distinguish in the field.	Deposited across numerous moraines, with several meltwater channels cutting through.	MIS 2
Intermediates	267	26.0	8.0	30–80	Boulder density is much less than the other EBTs, so the boulders were not studied further.	Lies across several moraines.	Possibly relates to more than one glacial limit
SSb 1	476	15.0	4.0	0–80	Boulder density varies, delimited to the north and south by the extent of kettle and kame drift.	Sits on a broad band of kettle and kame drift and continues eastward into the Atlantic Ocean.	MIS 10
RC 1	162	20.0	4.0	0–40	Boulder density varies, delimited to the north and south by the extent of kettle and kame drift. There are two tight, linear clusters of boulders roughly 1.7 km long and 1.5 km long.	Sits on a broad band of kettle and kame drift and continues eastward into the Atlantic Ocean.	MIS 12

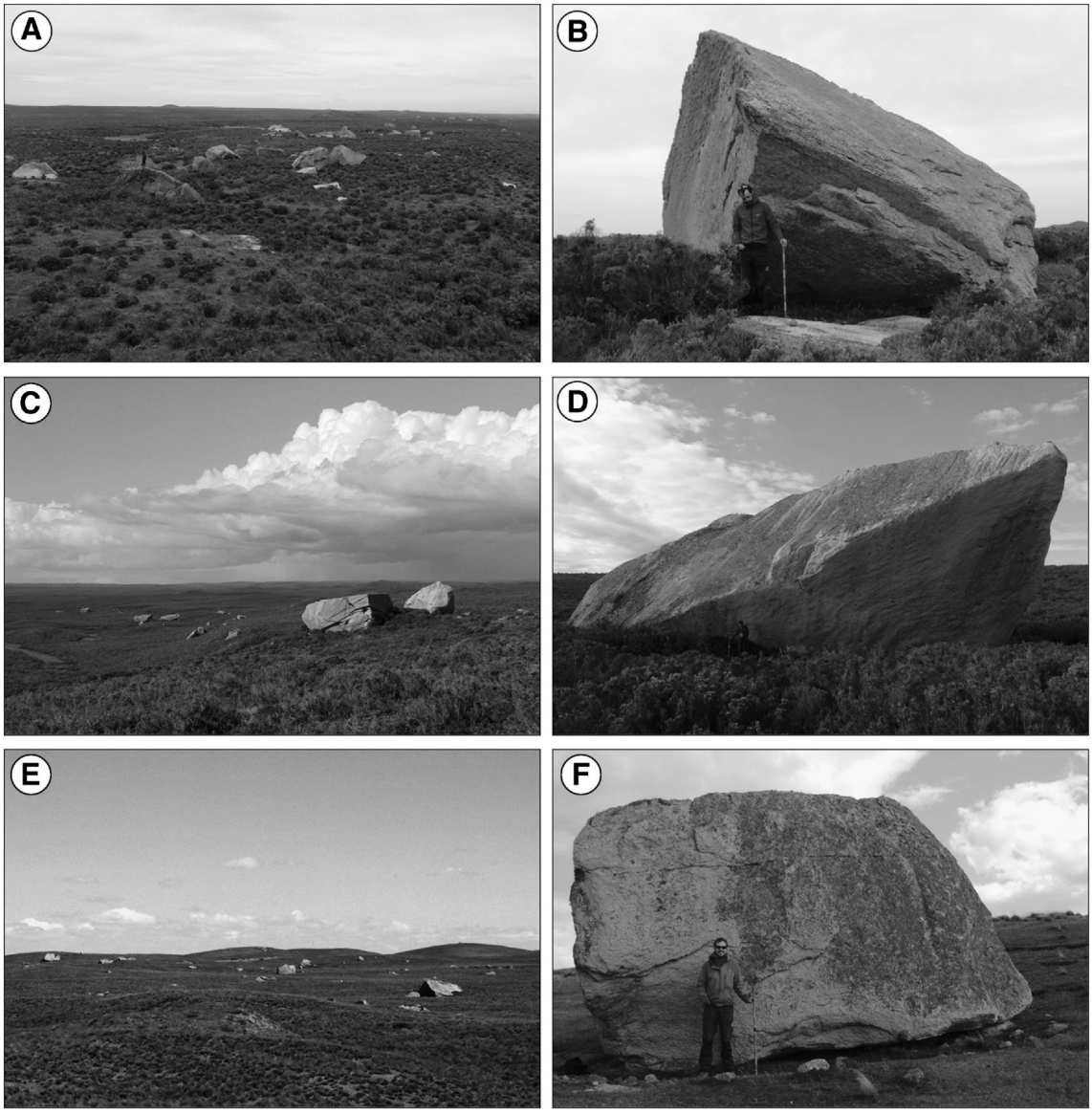

Fig. 7. Example photographs of the EBTs on Tierra del Fuego. (A) and (B) are from BI 1; (C) and (D) are from BI 2; and (E) and (F) are from RC 1. Note the large size, angularity, and clustering of the boulders. Additional colour photographs can be found in SM2.

angularity, and monolithology of the EBTs on Tierra del Fuego; and we suggest that these features match the characteristics expected of a supraglacial rock avalanche deposit (Shulmeister et al., 2009). Studies routinely estimate total rock avalanche deposit volumes of >1,000,000 m^3 (Shugar and Clague, 2011; Sosio et al., 2012; Delaney and Evans, 2014) and even >10,000,000 m^3 (Jibson et al., 2006; McColl and Davies, 2011; Shugar and Clague, 2011; Sosio et al., 2012), far in excess of our minimum estimates of >22,000 m^3 (or >150,000 m^3 assuming that the coarse fraction accounts for around 15% of the total volume; Delaney and Evans, 2014). This suggests that the size of the deposit is not unreasonable for a supraglacial rock avalanche. The clustering of the EBTs suggests that the erosion of the boulders occurred in discrete events and implies that gradual erosion at the source is improbable. Debuttressing during glacial retreat could have resulted in episodic deposition of debris caused by joint failures. However, we note that the boulders cut across a range of glacial geomorphology – both small moraine ridges and kettle and kame topography (Fig. 4) – and that the RC 1 EBT was deposited when the ice lobe was still fully extended. Additionally, whilst the EBTs might have been deposited during recession, they represent flowline features, not ice-marginal deposits.

The production of boulder trains as a result of supraglacial rock avalanches has not been explicitly examined in previous work. Shulmeister et al. (2009) noted that for large supraglacial rock avalanches, a greater proportion of thicker debris remains on the glacier surface rather than being incorporated into the subglacial system, and a characteristic 'carapace' of coarser debris generally caps deposits (Reznichenko et al., 2011). Coarse distal rims are found in numerous deposits (Hewitt, 1999, 2009; Chevalier et al., 2009; McColl and Davies, 2011; Shugar and Clague, 2011), and theoretically, these could result in boulder trains, especially if divergent flowlines drew the boulders into a train prior to deposition (Evenson et al., 2009). However, large boulders may also be found across the debris sheet, with the rim simply representing a greater density of large boulders caused by bulldozing (Shugar and Clague, 2011). It thus remains unclear exactly how a rock avalanche debris sheet is transformed into EBTs, but we now discuss a conceptual model for their transport and deposition.

5.2. Transport and deposition

The lateral position of the EBTs on Tierra del Fuego probably resulted from ice to the north (the Magellan lobe) deflecting the BI–SSb lobe to

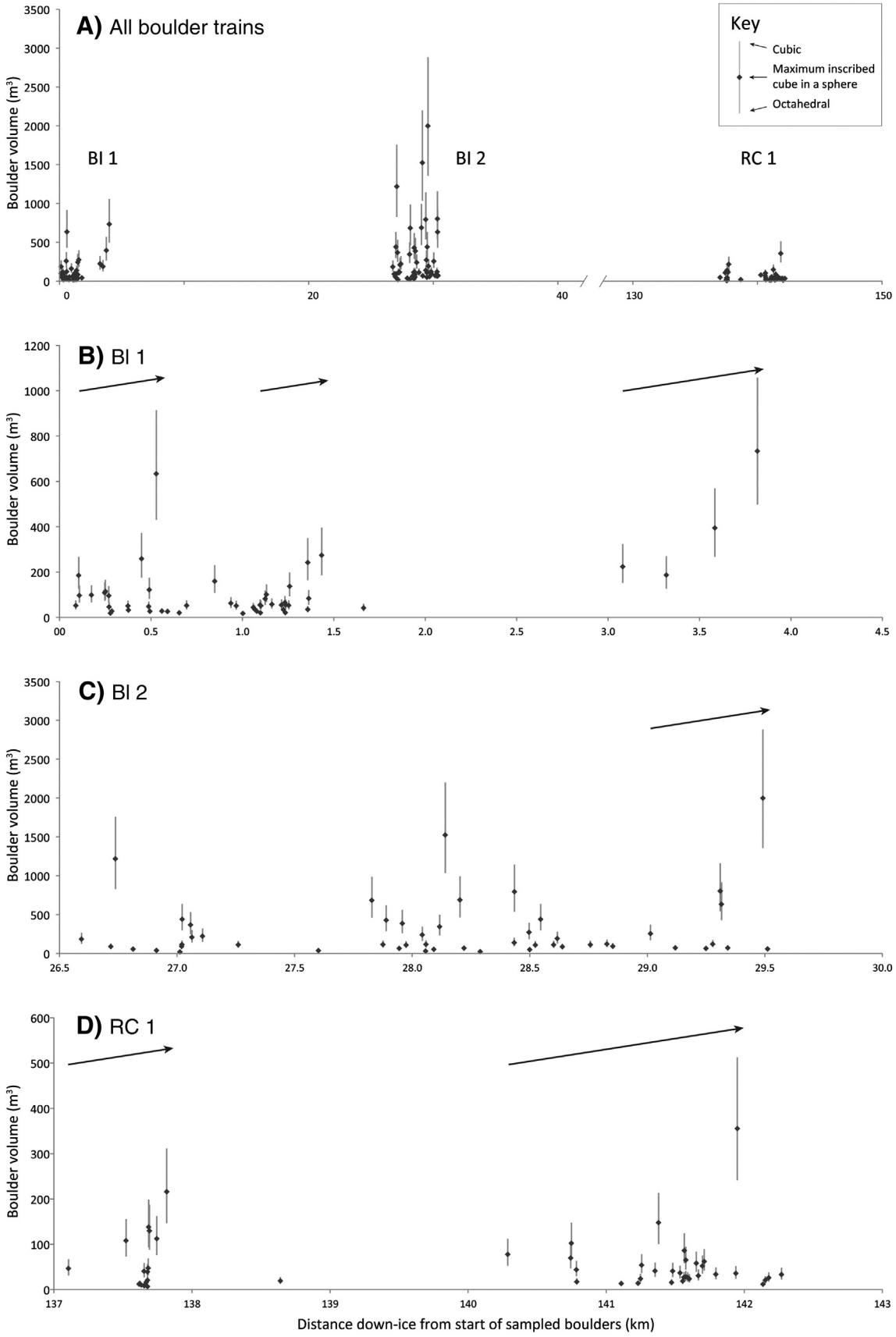

Fig. 8. The results of boulder volume measurements. (A) Shows the results for all three boulder trains, which are shown individually beneath: (B) BI 1; (C) BI 2; (D) RC 1. Arrows highlight an apparent repeated pattern of increasing down-ice volume across several near-consecutive boulders in all three EBTs.

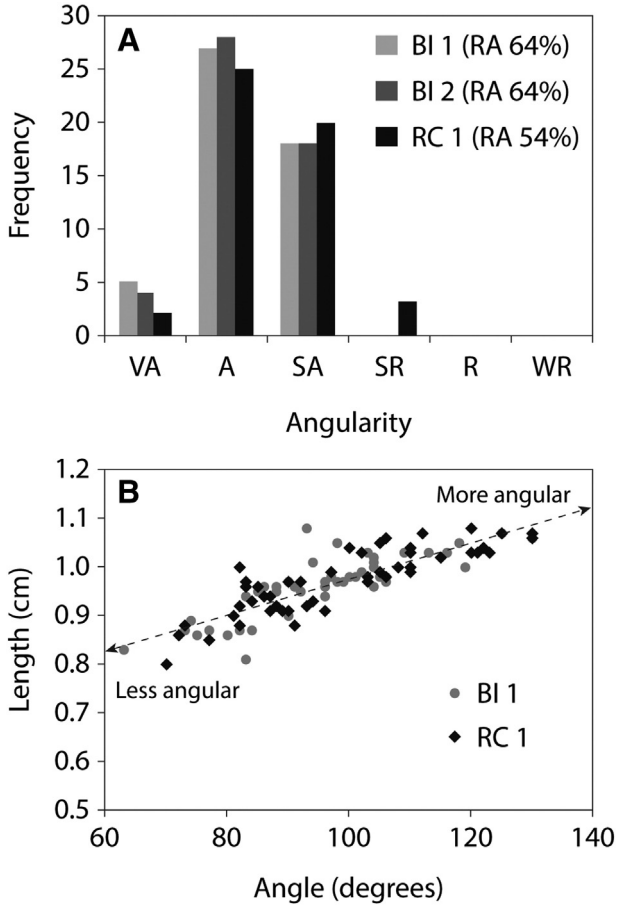

Fig. 9. The results of angularity measurements. (A) Is a frequency histogram of observed boulder roundness based on criteria in SM1.1, showing a dominance of angular boulders supported by high RA values (percentage of angular and very angular boulders). (B) Shows the similarity in boulder edge roundness between BI 1 and RC 1.

the east (Fig. 3), with divergent flow lines focusing the boulders in a lateral position (Evenson et al., 2009). Thus we envisage that the boulders were transported supraglacially from the central Cordillera Darwin, east of Isla Dawson, before turning sharply east into Bahía Inútil to be deposited on the south side of the former ice lobe (Fig. 3). Given that the Cordillera Darwin has experienced seismic activity in the past (Cunningham, 1993; Klepeis, 1994; Bentley and McCulloch, 2005), the four distinct boulder trains may logically have resulted from separate rock avalanche pulses (Larsen et al., 2005; Jibson et al., 2006). Ice crevassing, subaerial weathering, and meltwater may have acted to remove much of the finer material (Shulmeister et al., 2009), and ice flow and the divergence of flow lines then dragged the distal rim and boulder carapace into trains (Evenson et al., 2009).

Our mapping shows that the EBTs are significantly more extensive than previously thought (Evenson et al., 2009) and occur at several places along the southern limit of the former ice lobe. There are also numerous boulders that do not cluster as boulder trains (intermediates) but act as a continuum between BI 1/BI 2 and SSb 1/RC 1. Whilst the EBTs may represent distinct spatial and temporal events (as proposed by Kaplan et al., 2007, and Evenson et al., 2009), they could also represent rock avalanche pulses during the same period, possibly linked to seismic activity (Larsen et al., 2005; Chevalier et al., 2009). Studies in New Zealand have suggested that supraglacial rock avalanches may result in the deposition of nonclimatic moraines (Anderson and Mackintosh, 2006; Tovar et al., 2008; Shulmeister et al., 2009; Reznichenko et al., 2011). However, given the small area and isolated nature of the EBTs compared to the area covered by the BI–SSb ice lobe, a similar debris-induced, nonclimatic model is improbable.

The patterns of increasing down-ice boulder volume observed within each of the EBTs (Fig. 8) are unlikely to have been preserved in any scenario other than deposition onto – and transport on top of – the former ice. However, the formation of these patterns is unclear. Little evidence suggests that gravitational sorting of avalanche debris occurs (Marangunic and Bull, 1968; Shugar and Clague, 2011), but Hewitt (2009), Shugar and Clague (2011), and Delaney and Evans (2014) described trains of debris several metres wide and parallel to the direction of debris flow. These likely resulted from snow ploughing of a large boulder, with finer material following behind on exposed glacial ice (Delaney and Evans, 2014), and currently offer the best analogue for the patterns of boulder size trends seen in Tierra del Fuego.

5.3. Rock surface weathering

The Schmidt hammer data show a statistical difference between the RC 1 and BI 1 EBTs, indicating that the RC 1 boulders have been subjected to a greater degree of weathering than the BI 1 boulders. However, the differences are not as great as might be expected if intense, episodic erosion has taken place (Table 2). The *R*-values showed a total average difference of 5.9, whereas McCarroll and Nesje (1993) demonstrated differences of 25–40 between Little Ice Age and Late Glacial sites in western Norway; and Matthews and Owen (2010) highlighted differences of 21–35 between Little Ice Age and Preboreal sites in southern Norway. Rock weathering (and therefore *R*-values) could have reached saturation in Tierra del Fuego. However, despite agreement that *R*-values will progress toward a dynamic equilibrium over time (White et al., 1998; Engel, 2007; Sánchez et al., 2009; Černá and Engel, 2011; Stahl et al., 2013), numerous studies have effectively distinguished LGM and pre-LGM deposits using the technique on timescales of 10s to 100 s ka (Ballantyne et al., 1997; Rae et al., 2004; Černá and Engel, 2011; Stahl et al., 2013). Very high rates of weathering are required to reduce the ages of the RC 1 boulders (Table 2), yet no obvious jump in *R*-values occurs between these and the BI 1/BI 2 boulder trains.

The roughness data show a statistical difference between the total values RC 1 and BI 1/BI 2, but also between the BI 1 and BI 2 total values. Because BI 1 and BI 2 are assumed to be roughly the same age (lying within the same ice marginal deposits; Fig. 3), this implies that the difference between RC 1 and BI 1/BI 2 is not necessarily related to a significant difference in age. Differences between BI 1 and BI 2 could be driven by the highly variable values measured for the top aspect faces of the boulders, but statistical similarities also exist between the BI 1/BI 2 and RC 1 aspect faces, suggesting that any differences are unlikely to be the result of a great difference in age between these EBTs. Most importantly, and like the Schmidt hammer data, we do not find a jump in values between RC 1 and BI 1/BI 2 that might be expected if intense, episodic erosion has taken place (Table 2). The average total difference in roughness between RC 1 and BI 2 is 0.5 mm at the 32-mm wavelength. Given that the large crystal size is >20 mm and that the averages for all three boulder trains are between 2.3 and 2.8 mm, this difference is negligible. McCarroll and Nesje (1996) recorded much greater differences in roughness values when studying salt spray and chemical weathering of boulders. We cannot directly compare studies of different lithologies in different environments, but we would expect a clear difference in roughness values between the RC 1 and BI 1/BI 2 boulder trains if intense erosion has occurred.

Kaplan et al. (2007) suggested that proximity to the coastline may have caused higher rates of salt-spray weathering of the RC 1 boulders. Similarly, the dominant effect of the westerly winds in the region could have caused increased aeolian abrasion. Fig. 12 shows the results for averaged rock surface hardness and rock surface roughness from each boulder, with total boulder values and east/west faces shown. Correlations between these results and the distance from the start of the BI 1 and RC 1 boulder trains are negligible. Given the variability in the data, there is no indication that salt-spray weathering or aeolian

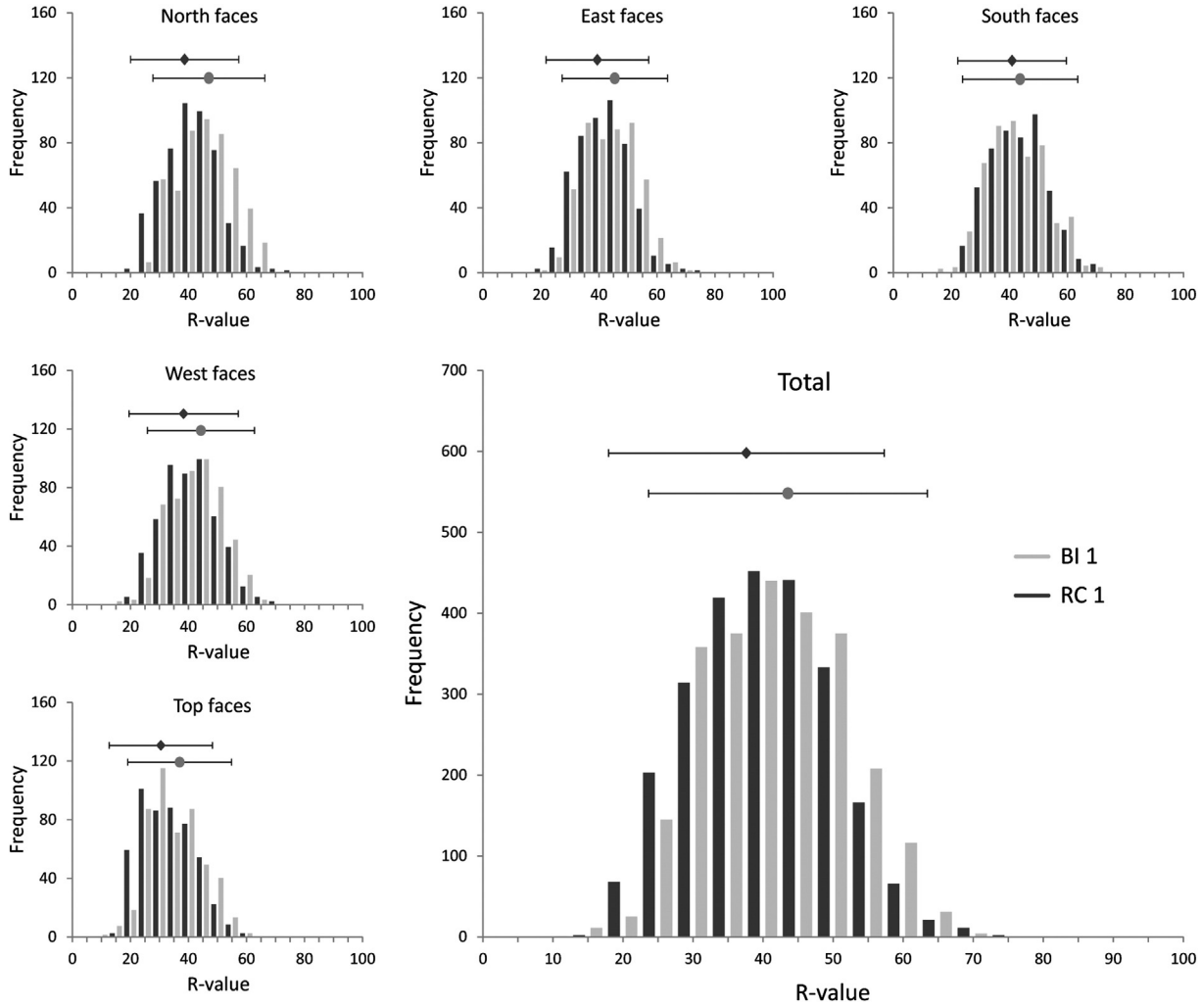

Fig. 10. Results of Schmidt hammer rock hardness analysis on the BI 1 and RC 1 EBTs, as total data and split into directional faces. Mean data are shown with 2σ errors, in addition to frequency histograms that illustrate the overlap between the two boulder trains.

abrasion has had a variable effect on boulders within RC 1 or a markedly greater effect on RC 1 than BI 1.

Weathering could have been operating on a scale greater than that recorded by our proxies, but whilst examples of microgullies and potholes are abundant on the top surfaces of the RC 1 boulders (Kaplan et al., 2007), similar features exist on the BI 1 and BI 2 boulders, we found little difference in top surface weathering between the boulder trains (see SM2). The similarity in weathering results between the EBTs suggests that they have probably experienced similar local climatic conditions. This is important given that the intense weathering needed to reduce the ages of the RC 1 boulder train during, or since, the LGM should have also reduced the ages of the BI 1 and BI 2 boulder trains. The cosmogenic exposure dates for the BI 1 and BI 2 boulder trains are believed to be good estimates of the time of deposition (around the LGM), agreeing with radiocarbon dates in the area (Heusser, 2003; McCulloch et al., 2005; Kaplan et al., 2008; Hall et al., 2013), so factors that reduced the RC 1 boulder dates by hundreds of thousands of years are highly unlikely to have also reduced the BI 1 and BI 2 dates.

5.4. Alternative (post-)depositional model

The EBTs on Tierra del Fuego were thought to have been deposited during different glacial episodes (MIS 12, 10, and 2), but cosmogenic nuclide exposure dating from all of the EBTs yielded dates predominantly around 21 ka (Kaplan et al., 2007; Evenson et al., 2009). One hypothesis (the boulders are 'old') explains this anomaly by invoking intensive post-depositional exhumation and erosion of the RC 1 boulders (Kaplan et al., 2007), but a second (the boulders are 'young') suggests that supraglacial debris may have an inheritance signature. Our study demonstrates that the distribution, volume, and monolithology of the boulder trains are indicative of supraglacial transport of rock avalanche material, and our rock surface weathering data does not support intensive post-depositional exhumation and erosion of the RC 1 boulders. Given this information, our data support the second, 'young' hypothesis, whereby the EBTs were transported and deposited at roughly the same time (i.e. within a few thousands of years, rather than separated by 100 s of thousands of years). Under this scenario, one would anticipate mostly young ages from the boulders, but with some anomalously old dates resulting from an inheritance signal owing to pre-exposure of boulders in the cliff face, which were not then sufficiently eroded during supraglacial transport (Applegate et al., 2010, 2012; Heyman et al., 2011).

This scenario is similar to that envisaged for the Foothills boulder train in Alberta, where Jackson et al. (1997) suggested that an erratic boulder that yielded a date of ca. 53 ka (four times older than the next oldest date) was improbable and most likely caused by pre-exposure prior to glacial transport. This implies that, for a supraglacial EBT deposit, a fraction of boulders should be expected to yield anomalously old dates. Assuming that the majority of ^{10}Be cosmogenic exposure dates are roughly correct, three anomalously old dates are apparent from the Tierra del Fuego boulder trains (Kaplan et al., 2007; Evenson et al., 2009). For RC 1, one date (ca. 57 ka) out of 7 and for BI 2, one date

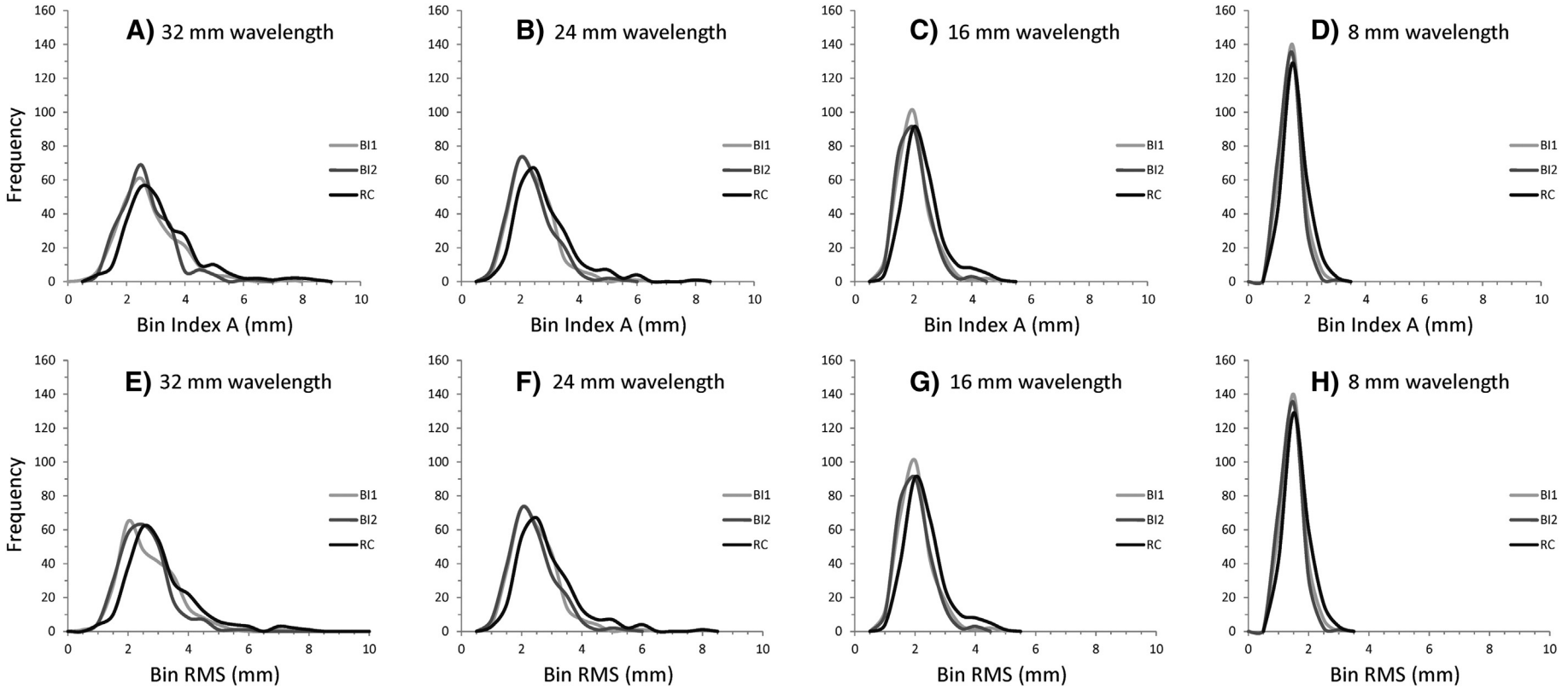

Fig. 11. Results of profile gauge rock surface roughness analysis on the BI 1, BI 2, and RC 1 EBTs, shown as frequency distributions. (A–D) are Index A results and (E–H) are RMS results. Note the similarity between the results of the two methods. RMS data is used in this study, focussing on the 32-mm wavelength.

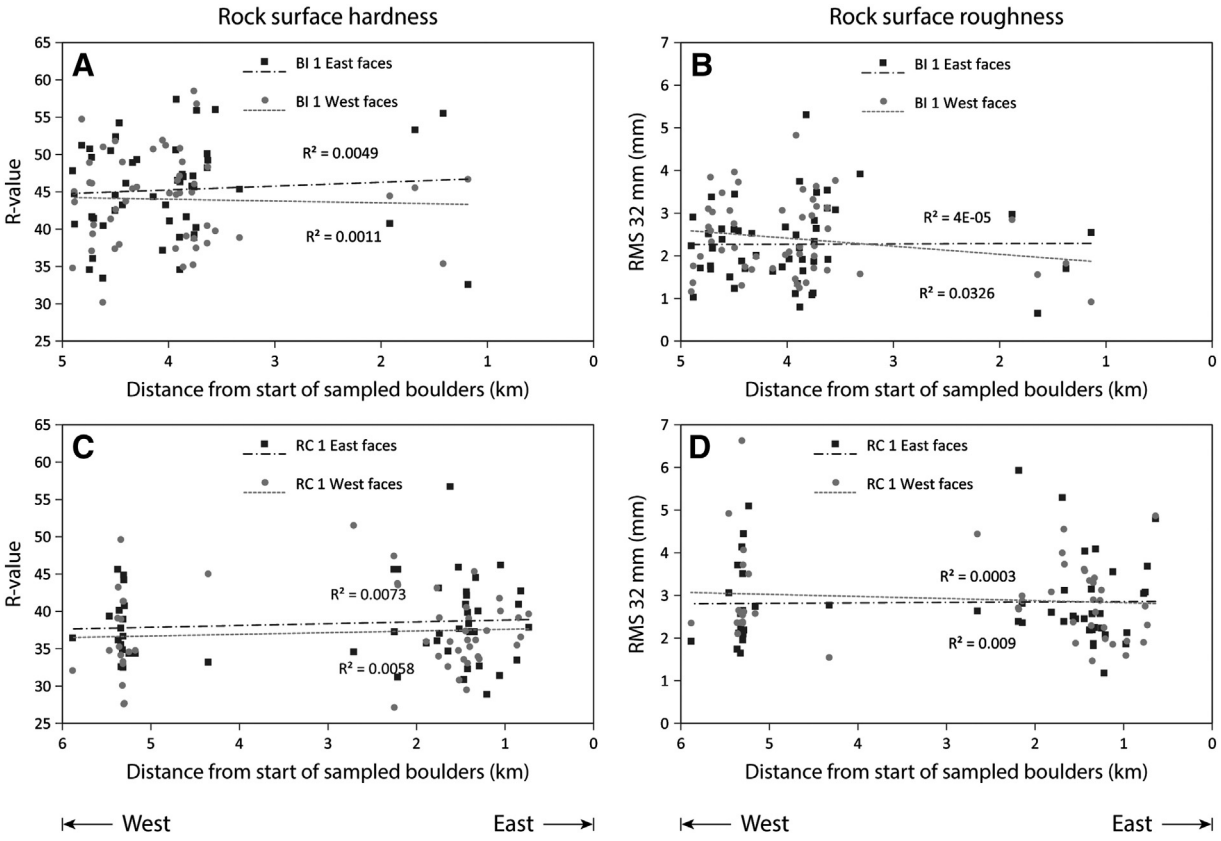

Fig. 12. The rock surface hardness and roughness results from Figs. 11 and 12 plotted to illustrate variations in aspect with distance along the boulder trains (data points relate to individual boulders and are only shown for BI 1 and RC 1). (A) Shows hardness results for the east and west faces of BI 1, and (B) shows roughness results for the east and west faces of BI 1. (C) Shows hardness results for the east and west faces of RC 1, and (D) shows roughness results for the east and west faces of RC 1. In all graphs, boulder values toward the right are located farther to the east and those toward the left are located farther to the west. No discernible trends are found in either of the boulder trains, as illustrated by very low R^2 values, suggesting that salt weathering has not affected RC 1 significantly more than BI 1, as hypothesised by Kaplan et al. (2007), despite closer proximity to the coast.

(ca. 56 ka) out of 17 may have been pre-exposed. The similarity between these ages could indicate a consistent (pre-)exposure pattern, but more samples would be needed to support this idea. The outlier from SSb 1 is significantly older at ca. 222 ka, although this is only one of two samples from that boulder train.

Leaving aside the anomalously old dates, substantial variability remains in the cosmogenic nuclide exposure dates of the RC 1 EBT, a fact that Kaplan et al. (2007) highlighted. Variability in the dates could have been caused by variability in the residence time on the ice during transport. Hubbard et al. (2005) modelled ice flow velocities of up to 2000 m a^{-1} for the northern Patagonian Ice Sheet. Assuming similar velocities and a transport distance of up to 250 km for the BI–SSb lobe, transport time may have been as little as 0.125 ka: insignificant given dating uncertainty. Slower velocities of 100 m a^{-1} or even 50 m a^{-1} would have resulted in residence times of 2.5 or 5 ka, respectively; but given that the clustering of the EBTs suggests that they were deposited as discrete events, this could only have resulted in age differences between, not within, boulder trains.

Rather, we suggest three mechanisms that could have produced the variability in RC 1. Firstly, RC 1 has probably experienced greater erosion than BI 1/BI 2 as it was deposited first, causing variable reduction in cosmogenic nuclide exposure dates. Second, we agree with Kaplan et al. (2007) that many boulders in the RC 1 train show signs of surface weathering, though we find similar signs in the BI 1/BI 2 EBTs. Sampling of the RC 1 boulder train may have been more affected by weathered surfaces than BI 1/BI 2 because fewer larger boulders are found in RC 1 and this could have resulted in sampling of boulders that were 'less ideal' than those in the other boulder trains.

Third, Jackson et al. (1997) suggested that boulder orientation can affect the spread of dates in a boulder train. We have demonstrated that all boulders in Tierra del Fuego are likely 'at rest', but do not know how long they were sitting on melting ice before reaching this state. The RC 1 and SSb 1 boulder trains are located on large bands of kettle kame drift, a characteristic deposit of 'dead ice' terrain (Dyke and Evans, 2005; Schomacker, 2008), whereas BI 1 and BI 2 are located on small, sharp moraines interspersed by meltwater channels. Ground ice within the kettle and kame topography could have taken a long time to fully melt and settle, and occasional examples of boulders exposed at the coastline within the kettle and kame deposits may be a result of this slow process of settling (see SM2). Thus, the RC 1 boulder train may have taken ca. 10 ka to come to rest and implies that ground ice melting may have prevailed long after the recession of the ice lobe.

To summarise, the main implication behind this alternative history of the EBTs on Tierra del Fuego is that the established age model for the timing of glaciations in the region may need re-examining. Whilst this study provides a new approach to interpreting the cosmogenic nuclide exposure dates, further independent age controls for the glacial limits are needed to investigate the timing of glacial advances.

6. Conclusion

Erratic boulder trains make valuable targets for flow-line indicators and cosmogenic nuclide exposure dating, but few have been reported in detail and further studies are needed to understand their formation, transport, and deposition. Based on the limited number of EBTs that have been reported in the literature, we identify an apparent trend between boulder size, transport distance, and likely mode of transport. The EBTs containing boulders greater than ca. 5 m in diameter and/or demonstrating transport from the source lithology of greater than ca. 10 km are likely to have been transported supraglacially.

In Tierra del Fuego, the distribution and volume of three boulder trains suggest that they were formed by a rock avalanche and transported and deposited supraglacially. This highlights a former ice flow line from the Cordillera Darwin and helps to constrain the position of ice divides and maximum ice surface elevation. Using a variety of techniques and measurements, we do not identify any major changes in rock surface weathering characteristics across EBTs that have been previously interpreted to be from different glacial cycles. Thus we suggest that they are much closer in age (probably within a few thousand years), which is also consistent with previous cosmogenic nuclide exposure dates from the boulders. Occasional, anomalously old samples should be expected from supraglacial boulder trains caused by pre-exposure prior to and during glacial transport, and an understanding of the likely history of an EBT should be an integral part of using the features for dating.

Acknowledgements

We are very grateful to William Christiansen, Harold Lovell, Mark Hulbert, and Paul Lincoln for their fantastic assistance during field work. The research was primarily funded by a UK NERC PhD studentship awarded to CMD at Durham University, but was also supported by an Explorers Club Exploration Grant, Quaternary Research Association New Research Workers' Award, Santander Mobility Grant, the Durham University Faculty of Social Sciences and Health, and Durham University Geography Department. Thanks to Jorge Rabassa and Andrea Coronato at CADIC-CONICET in Ushuaia, Juan Carlos Aravena at CEQUA in Punta Arenas, the Fernandez family of Estancia San Clemente, the Vilamera family of Estancia Sara, and Juan Robertson of Estancia Tres Hermanos for their assistance. This paper has benefitted greatly from the insightful comments of three anonymous reviewers and the editor, Richard Marston.

Appendix A. Supplementary data

Supplementary data to this article can be found online at http://dx.doi.org/10.1016/j.geomorph.2014.09.017.

References

Adamson, D., Colhoun, E., 1992. Late Quaternary glaciation and deglaciation of the Bunger Hills, Antarctica. Antarct. Sci. 4, 435–446.
Anderson, B., Mackintosh, A., 2006. Temperature change is the major driver of late-glacial and Holocene glacier fluctuations in New Zealand. Geology 34, 121–124. http://dx.doi.org/10.1130/g22151.1.
Applegate, P.J., Urban, N.M., Laabs, B.J.C., Keller, K., Alley, R.B., 2010. Modeling the statistical distributions of cosmogenic exposure dates from moraines. Geosci. Model Dev. 3, 293–307.
Applegate, P.J., Urban, N.M., Keller, K., Lowell, T.V., Laabs, B.J.C., Kelly, M.A., Alley, R.B., 2012. Improved moraine age interpretations through explicit matching of geomorphic process models to cosmogenic nuclide measurements from single landforms. Quat. Res. 77, 293–304. http://dx.doi.org/10.1016/j.yqres.2011.12.002.
Atkins, C.B., Barrett, P.J., Hicock, S.R., 2002. Cold glaciers erode and deposit: evidence from Allan Hills, Antarctica. Geology 30, 659–662. http://dx.doi.org/10.1130/0091-7613((2002) 030 < 0659:cgeade > 2.0.co;2).
Augustinus, P.C., Gore, D.B., Leishman, M.R., Zwartz, D., Colhoun, E.A., 1997. Reconstruction of ice flow across the Bunger Hills, East Antarctica. Antarct. Sci. 9, 347–354.
Ballantyne, C.K., McCarroll, D., Nesje, A., Dahl, S.O., 1997. Periglacial trimlines, former nunataks and the altitude of the last ice sheet in Wester Ross, northwest Scotland. J. Quat. Sci. 12, 225–238.
Benn, D.I., 2004. Clast morphology. In: Evans, D.J.A., Benn, D.I. (Eds.), A Practical Guide to the Study of Glacial Sediments. Arnold, London, pp. 78–92.
Bentley, M.J., McCulloch, R.D., 2005. Impact of neotectonics on the record of glacier and sea level fluctuations, Strait of Magellan, southern Chile. Phys. Geogr. 87A, 393–402. http://dx.doi.org/10.1111/j.0435-3676.2005.00265.x.
Bentley, M.J., Sugden, D.E., Hulton, N.R.J., McCulloch, R.D., 2005. The landforms and pattern of deglaciation in the Strait of Magellan and Bahia Inútil, southernmost South America. Phys. Geogr. 87A, 313–333. http://dx.doi.org/10.1111/j.0435-3676.2005.00261.x.
Boulton, G.S., 1978. Boulder shapes and grain-size distributions of debris as indicators of transport paths through a glacier and till genesis. Sedimentology 25, 773–799. http://dx.doi.org/10.1111/j.1365-3091.1978.tb00329.x.
Boulton, G.S., 1996. Theory of glacial erosion, transport and deposition as a consequence of subglacial sediment deformation. J. Glaciol. 42, 43–62.
Černá, B., Engel, Z., 2011. Surface and sub-surface Schmidt hammer rebound value variation for a granite outcrop. Earth Surf. Process. Landf. 36, 170–179. http://dx.doi.org/10.1002/esp.2029.
Chevalier, G., Davies, T., McSaveney, M., 2009. The prehistoric Mt Wilberg rock avalanche, Westland, New Zealand. Landslides 6, 253–262. http://dx.doi.org/10.1007/s10346-009-0156-5.
Coronato, A., Roig, C., Rabassa, J., Meglioli, A., 1999. Erratic boulder field of pre-Illinoian age at Punta Sinaí, Tierra del Fuego, southernmost South America. XV INQUA International Congress, Durham, South Africa, pp. 47–48.
Coronato, A., Martínez, O., Rabassa, J., 2004. Glaciations in Argentine Patagonia, southern South America. In: Ehlers, J., Gibbard, P.L. (Eds.), Developments in Quaternary Sciences. Elsevier, pp. 49–67 http://dx.doi.org/10.1016/s1571-0866(04)80111-8.
Cunningham, W.D., 1993. Strike-slip faults in the southernmost andes and the development of the Patagonian orocline. Tectonics 12, 169–186. http://dx.doi.org/10.1029/92tc01790.
Darvill, C.M., Stokes, C.R., Bentley, M.J., Lovell, H., 2014. A glacial geomorphological map of the southernmost ice lobes of Patagonia: the Bahía Inútil–San Sebastián, Magellan, Otway, Skyring and Río Gallegos lobes. J. Map. 1–21 http://dx.doi.org/10.1080/17445647.2014.890134.
Darwin, C., 1841. On the distribution of the erratic boulders and on the contemporaneous unstratified deposits of South America. Trans. Geol. Soc. London 2–6, 415–431. http://dx.doi.org/10.1144/transgslb.6.2.415.
Davies, B.J., Glasser, N.F., Carrivick, J.L., Hambrey, M.J., Smellie, J.L., Nývlt, D., 2013. Landscape evolution and ice-sheet behaviour in a semi-arid polar environment: James Ross Island, NE Antarctic Peninsula. Geol. Soc. Lond., Spec. Publ. 381, 353–395. http://dx.doi.org/10.1144/sp381.1.
Davis, J.W., 1880. On a group of erratic boulders at Norber, near Clapham, in Yorkshire. Proc. Yorks. Geol. Polytech. Soc. 7, 266–273. http://dx.doi.org/10.1144/pygs.7.3.266.
Delaney, K., Evans, S., 2014. The 1997 Mount Munday landslide (British Columbia) and the behaviour of rock avalanches on glacier surfaces. Landslides 1–18 http://dx.doi.org/10.1007/s10346-013-0456-7.
DiLabio, R.N.W., 1981. Glacial dispersal of rocks and minerals at the south end of Lac Mistassini, Quebec, with special reference to the Icon dispersal train. Geol. Surv. Can. Bull. 323, 46.
DiLabio, R.N.W., 1990. Glacial dispersal trains. In: Kujansuu, R., Saarnisto, M. (Eds.), Glacial Indicator Tracing. Balkema Publishers, Rotterdam, Netherlands, pp. 109–122.
Dyke, A.S., Evans, D.J.A., 2005. Ice-marginal terrestrial landsystems: Northern Laurentide and Innuitian ice sheet margins. In: Evans, D.J.A. (Ed.), Glacial Landsystems. Hodder Arnold, London.
Dyke, A.S., Morris, T.F., 1988. Drumlin fields, dispersal trains, and ice streams in Arctic Canada. Can. Geogr. 32, 86–90.
Engel, Z., 2007. Measurement and age assignment of intact rock strength in the Krkonoše Mountains, Czech Republic. Z. Geomorphol. 51, 69–80. http://dx.doi.org/10.1127/0372-8854/2007/0051s-0069.
Evans, D.J.A., 2007. Glacial erratics and till dispersal indicators. In: Elias, S.A. (Ed.), Encyclopedia of Quaternary Science. Elsevier, Oxford, pp. 975–978 http://dx.doi.org/10.1016/B0-44-452747-8/00089-2.
Evenson, E.B., Burkhart, P.A., Gosse, J.C., Baker, G.S., Jackofsky, D., Meglioli, A., Dalziel, I., Kraus, S., Alley, R.B., Berti, C., 2009. Enigmatic boulder trains, supraglacial rock avalanches, and the origin of "Darwin's boulders," Tierra del Fuego. GSA Today 19, 4–10. http://dx.doi.org/10.1130/GSATG72A.1.
Goldie, H.S., 2005. Erratic judgements: re-evaluating solutional erosion rates of limestones using erratic-pedestal sites, including Norber, Yorkshire. Area 37, 433–442. http://dx.doi.org/10.1111/j.1475-4762.2005.00653.x.
Goudie, A.S., 2006. The Schmidt Hammer in geomorphological research. Prog. Phys. Geogr. 30, 703–718. http://dx.doi.org/10.1177/0309133306071954.
Hall, B.L., Porter, C.T., Denton, G.H., Lowell, T.V., Bromley, G.R.M., 2013. Extensive recession of Cordillera Darwin glaciers in southernmost South America during Heinrich Stadial 1. Quat. Sci. Rev. 62, 49–55. http://dx.doi.org/10.1016/j.quascirev.2012.11.026.
Heusser, C.J., 2003. Ice Age Southern Andes: A Chronicle of Paleoecological Events. Elsevier http://dx.doi.org/10.1016/S1571-0866(03)80001-5.
Hewitt, K., 1999. Quaternary moraines vs catastrophic rock avalanches in the Karakoram Himalaya, Northern Pakistan. Quat. Res. 51, 220–237. http://dx.doi.org/10.1006/qres.1999.2033.
Hewitt, K., 2009. Rock avalanches that travel onto glaciers and related developments, Karakoram Himalaya, Inner Asia. Geomorphology 103, 66–79. http://dx.doi.org/10.1016/j.geomorph.2007.10.017.
Heyman, J., Stroeven, A.P., Harbor, J.M., Caffee, M.W., 2011. Too young or too old: evaluating cosmogenic exposure dating based on an analysis of compiled boulder exposure ages. Earth Planet. Sci. Lett. 302, 71–80. http://dx.doi.org/10.1016/j.epsl.2010.11.040.
Hubbard, A., Hein, A.S., Kaplan, M.R., Hulton, N.R.J., Glasser, N., 2005. A modelling reconstruction of the last glacial maximum ice sheet and its deglaciation in the vicinity of the Northern Patagonian Icefield, South America. Phys. Geogr. 87A, 375–391. http://dx.doi.org/10.1111/j.0435-3676.2005.00264.x.
Huddart, D., 2002. Norber erratics. In: Huddart, D., Glasser, N. (Eds.), Quaternary of Northern England. JNCC, Peterborough, pp. 200–203.
Jackson, L.E., Duk-Rodkin, A., 1996. Quaternary geology of the ice-free corridor: glacial controls on the peopling of the New World. In: Akazawa, T., Szathmary, E. (Eds.), Prehistoric Mongoloid Dispersals. Oxford University Press, Oxford, pp. 214–227.
Jackson, L.E., Little, E.C., 2004. A single continental glaciation of Rocky Mountain Foothills, south-western Alberta, Canada. In: Ehlers, J., Gibbard, P.L. (Eds.), Developments in Quaternary Sciences. Elsevier, pp. 29–38 http://dx.doi.org/10.1016/S1571-0866(04)80183-0.
Jackson, L.E., Phillips, F.M., Shimamura, K., Little, E.C., 1997. Cosmogenic ^{36}Cl dating of the Foothills erratics train, Alberta, Canada. Geology 25, 195–198. http://dx.doi.org/10.1130/0091-7613 ((1997)025<0195:ccdotf>2.3.co;2).

Jackson, L.E., Phillips, F.M., Little, E.C., 1999. Cosmogenic ^{36}Cl dating of the maximum limit of the Laurentide Ice Sheet in southwestern Alberta. Can. J. Earth Sci. 36, 1347–1356. http://dx.doi.org/10.1139/e99-038.

Jibson, R.W., Harp, E.L., Schulz, W., Keefer, D.K., 2006. Large rock avalanches triggered by the M 7.9 Denali Fault, Alaska, earthquake of 3 November 2002. Eng. Geol. 83, 144–160. http://dx.doi.org/10.1016/j.enggeo.2005.06.029.

Kaplan, M.R., Douglass, D.C., Singer, B.S., Caffee, M.W., 2005. Cosmogenic nuclide chronology of pre-last glacial maximum moraines at Lago Buenos Aires, 46 degrees S, Argentina. Quat. Res. 63, 301–315. http://dx.doi.org/10.1016/j.yqres.2004.12.003.

Kaplan, M.R., Coronato, A., Hulton, N.R.J., Rabassa, J.O., Kubik, P.W., Freeman, S.P.H.T., 2007. Cosmogenic nuclide measurements in southernmost South America and implications for landscape change. Geomorphology 87, 284–301. http://dx.doi.org/10.1016/j.geomorph.2006.10.005.

Kaplan, M.R., Fogwill, C.J., Sugden, D.E., Hulton, N., Kubik, P.W., Freeman, S.P.H.T., 2008. Southern Patagonian glacial chronology for the Last Glacial period and implications for Southern Ocean climate. Quat. Sci. Rev. 27, 284–294. http://dx.doi.org/10.1016/j.quascirev.2007.09.013.

Kirkbride, M.P., 2005. Boulder edge-roundness as an indicator of relative age: a lochnagar case study. Scott. Geogr. J. 121, 219–236. http://dx.doi.org/10.1080/00369220518737232.

Klepeis, K.A., 1994. Relationship between uplift of the metamorphic core of the southernmost Andes and shortening in the Magallanes foreland fold and thrust belt, Tierra del Fuego, Chile. Tectonics 13, 882–904. http://dx.doi.org/10.1029/94tc00628.

Knechtel, M.M., 1942. Snake Butte boulder train and related glacial phenomena, north-central Montana. Geol. Soc. Am. Bull. 53, 917–936. http://dx.doi.org/10.1130/gsab-53-917.

Kujansuu, R., Saarnisto, M., 1990. Glacial Indicator Tracing. Balkema Publishers, Rotterdam, Netherlands.

Lal, D., 1991. Cosmic ray labeling of erosion surfaces: in situ nuclide production rates and erosion models. Earth Planet. Sci. Lett. 104, 424–439. http://dx.doi.org/10.1016/0012-821X(91)90220-C.

Larsen, S.H., Davies, T.R.H., McSaveney, M.J., 2005. A possible coseismic landslide origin of late Holocene moraines of the Southern Alps, New Zealand. N. Z. J. Geol. Geophys. 48, 311–314. http://dx.doi.org/10.1080/00288306.2005.9515117.

Lawson, T.J., 1990. Former ice movement in Assynt, Sutherland, as shown by the distribution of glacial erratics. Scott. J. Geol. 26, 25–32. http://dx.doi.org/10.1144/sjg26010025.

Lawson, T.J., 1995. Boulder trains as indicators of former ice flow in Assynt, N.W. Scotland. Quat. Newsl. 75, 15–21.

Marangunic, C., Bull, C., 1968. The Landslide on the Sherman Glacier, The Great Alaska Earthquake of 1964–Hydrology. Pt. A. National Academy of Sciences, Washington, DC, pp. 383–394.

Matthews, J.A., Owen, G., 2010. Schmidt hammer exposure-age dating: developing linear age-calibration curves using Holocene bedrock surfaces from the Jotunheimen–Jostedalsbreen regions of southern Norway. Boreas 39, 105–115. http://dx.doi.org/10.1111/j.1502-3885.2009.00107.x.

McCarroll, D., 1991. The age and origin of Neoglacial moraines in Jotunheimen, southern Norway: new evidence from weathering-based data. Boreas 20, 283–295. http://dx.doi.org/10.1111/j.1502-3885.1991.tb00156.x.

McCarroll, D., Nesje, A., 1993. The vertical extent of ice sheets in Nordfjord, western Norway: measuring degree of rock surface weathering. Boreas 22, 255–265. http://dx.doi.org/10.1111/j.1502-3885.1993.tb00185.x.

McCarroll, D., Nesje, A., 1996. Rock surface roughness as an indicator of degree of rock surface weathering. Earth Surf. Process. Landf. 21, 963–977. http://dx.doi.org/10.1002/(sici)1096-9837((199610)21:10<963::aid-esp643>3.0.co;2-j).

McColl, S.T., Davies, T.R., 2011. Evidence for a rock-avalanche origin for 'The Hillocks' "moraine", Otago, New Zealand. Geomorphology 127, 216–224. http://dx.doi.org/10.1016/j.geomorph.2010.12.017.

McCulloch, R.D., Fogwill, C.J., Sugden, D.E., Bentley, M.J., Kubik, P.W., 2005. Chronology of the last glaciation in central Strait of Magellan and Bahia Inutil, southernmost South America. Phys. Geogr. 87A, 289–312. http://dx.doi.org/10.1111/j.0435-3676.2005.00260.x.

Meglioli, A., 1992. Glacial Geology and Chronology of southernmost Patagonia and Tierra del Fuego, Argentina and Chile(Ph.D. Thesis) Geology. Lehigh University.

Mountjoy, E.W., 1958. Jasper area Alberta, a source for the Foothills erratics train. Bull. Can. Petrol. Geol. 6, 218–226.

Natland, M., Gonzalez, P., Canon, A., Ernst, M., 1974. Geology and paleontology of Magellanes Basin: a system of stages for correlation of Magellanes Basin sediments. Mem. Geol. Soc. Am. 139, 3–57.

Nelson, E.P., Dalziel, I.W.D., Milnes, A.G., 1980. Structural geology of the Cordillera Darwin; collisional-style orogenesis in the southernmost Chilean Andes. Eclogae Geol. Helv. 73, 727–751.

Nesje, A., McCarroll, D., Dahl, S.O., 1994. Degree of rock surface weathering as an indicator of ice-sheet thickness along an east–west transect across southern Norway. J. Quat. Sci. 9, 337–347. http://dx.doi.org/10.1002/jqs.3390090404.

Putnam, A.E., Schaefer, J.M., Barrell, D.J.A., Vandergoes, M., Denton, G.H., Kaplan, M.R., Finkel, R.C., Schwartz, R., Goehring, B.M., Kelley, S.E., 2010. In situ cosmogenic ^{10}Be production-rate calibration from the Southern Alps, New Zealand. Quat. Geochronol. 5, 392–409. http://dx.doi.org/10.1016/j.quageo.2009.12.001.

Rabassa, J., 2008. Late Cenozoic glaciations in Patagonia and Tierra del Fuego. In: Rabassa, J. (Ed.), Developments in Quaternary Sciences. Elsevier, pp. 151–204 http://dx.doi.org/10.1016/s1571-0866(07)10008-7.

Rabassa, J., Coronato, A., MartÍNez, O., 2011. Late Cenozoic glaciations in Patagonia and Tierra del Fuego: an updated review. Biol. J. Linn. Soc. 103, 316–335. http://dx.doi.org/10.1111/j.1095-8312.2011.01681.x.

Rae, A.C., Harrison, S., Mighall, T., Dawson, A.G., 2004. Periglacial trimlines and nunataks of the Last Glacial Maximum: the Gap of Dunloe, southwest Ireland. J. Quat. Sci. 19, 87–97. http://dx.doi.org/10.1002/jqs.807.

Reznichenko, N.V., Davies, T.R.H., Alexander, D.J., 2011. Effects of rock avalanches on glacier behaviour and moraine formation. Geomorphology 132, 327–338. http://dx.doi.org/10.1016/j.geomorph.2011.05.019.

Roberts, D.H., Dackombe, R.V., Thomas, G.S.P., 2007. Palaeo-ice streaming in the central sector of the British–Irish Ice Sheet during the Last Glacial Maximum: evidence from the northern Irish Sea Basin. Boreas 36, 115–129. http://dx.doi.org/10.1111/j.1502-3885.2007.tb01186.x.

Roed, M.A., Mountjoy, E.W., Rutter, N.W., 1967. The Athabasca Valley Erratics Train, Alberta and Pleistocene ice movements across the continental divide. Can. J. Earth Sci. 4, 625–632. http://dx.doi.org/10.1139/e67-039.

Salonen, V.-P., 1986. Glacial Transport Distance Distributions of Surface Boulders in Finland. Geologian tutkimuskeskus.

Sánchez, J.S., Mosquera, D.F., Romaní, J.R.V., 2009. Assessing the age-weathering correspondence of cosmogenic ^{21}Ne dated Pleistocene surfaces by the Schmidt Hammer. Earth Surf. Process. Landf. 34, 1121–1125. http://dx.doi.org/10.1002/esp.1802.

Schomacker, A., 2008. What controls dead-ice melting under different climate conditions? A discussion. Earth Sci. Rev. 90, 103–113. http://dx.doi.org/10.1016/j.earscirev.2008.08.003.

Shakesby, R.A., Matthews, J.A., Karlén, W., Los, S.O., 2011. The Schmidt hammer as a Holocene calibrated-age dating technique: testing the form of the R-value-age relationship and defining the predicted-age errors. The Holocene 21, 615–628. http://dx.doi.org/10.1177/0959683610391322.

Shugar, D.H., Clague, J.J., 2011. The sedimentology and geomorphology of rock avalanche deposits on glaciers. Sedimentology 58, 1762–1783. http://dx.doi.org/10.1111/j.1365-3091.2011.01238.x.

Shulmeister, J., Davies, T.R., Evans, D.J.A., Hyatt, O.M., Tovar, D.S., 2009. Catastrophic landslides, glacier behaviour and moraine formation — a view from an active plate margin. Quat. Sci. Rev. 28, 1085–1096. http://dx.doi.org/10.1016/j.quascirev.2008.11.015.

Sosio, R., Crosta, G.B., Chen, J.H., Hungr, O., 2012. Modelling rock avalanche propagation onto glaciers. Quat. Sci. Rev. 47, 23–40. http://dx.doi.org/10.1016/j.quascirev.2012.05.010.

Stahl, T., Winkler, S., Quigley, M., Bebbington, M., Duffy, B., Duke, D., 2013. Schmidt hammer exposure-age dating (SHD) of late Quaternary fluvial terraces in New Zealand. Earth Surf. Process. Landf. 38, 1838–1850. http://dx.doi.org/10.1002/esp.3427.

Stalker, A.M., 1956. The erratics train, foothills of Alberta. Geol. Surv. Can. Bull. 37, 31.

Stalker, A.M., 1976. Megablocks, or the enormous erratics of the Albertan Prairies. Geol. Surv. Can. Pap. 76-1C, 185–188.

Stone, J.O., 2000. Air pressure and cosmogenic isotope production. J. Geophys. Res. 105, 23753–23759. http://dx.doi.org/10.1029/2000jb900181.

Tovar, S.D., Shulmeister, J., Davies, T.R., Geosci, Nature, 2008. Evidence for a landslide origin of New Zealand/'s Waiho Loop moraine. Nat. Geosci. 1, 524–526. http://dx.doi.org/10.1038/ngeo249.

Vincent, P.J., Wilson, P., Lord, T.C., Schnabel, C., Wilcken, K.M., 2010. Cosmogenic isotope (^{36}Cl) surface exposure dating of the Norber erratics, Yorkshire Dales: further constraints on the timing of the LGM deglaciation in Britain. Proc. Geol. Assoc. 121, 24–31. http://dx.doi.org/10.1016/j.pgeola.2009.12.009.

Ward, B.C., Bond, J.D., Gosse, J.C., 2007. Evidence for a 55–50 ka (early Wisconsin) glaciation of the Cordilleran ice sheet, Yukon Territory, Canada. Quat. Res. 68, 141–150. http://dx.doi.org/10.1016/j.yqres.2007.04.002.

White, K., Bryant, R., Drake, N., 1998. Techniques for measuring rock weathering: application to a dated fan segment sequence in southern Tunisia. Earth Surf. Process. Landf. 23, 1031–1043.

Wilson, P., Barrows, T.T., Lord, T.C., Vincent, P.J., 2012. Surface lowering of limestone pavement as determined by cosmogenic (^{36}Cl) analysis. Earth Surf. Process. Landf. 37, 1518–1526. http://dx.doi.org/10.1002/esp.3260.